Synthesis and alignment of liquid crystalline elastomers

Katie M. Herbert[1], *Hayden E. Fowler*[1], *Joselle M. McCracken*[1], *Kyle R. Schlafmann*[1], *Jeremy A. Koch*[1] *and Timothy J. White*[1,2]✉

Abstract | Liquid crystalline elastomers (LCEs) are crosslinked polymer networks that combine the elastic properties of rubber with the anisotropic properties of liquid crystals. Multifunctionality and responsivity can be programmed into LCEs by patterning their local orientation, which is difficult to achieve in other monolithic material systems. Advances in the synthesis and alignment of LCEs have paved the way for their functional integration in robotics, optics, consumer products, energy and healthcare devices. In this Review, we discuss recent advances in materials chemistry and processing that have contributed to the resurgence in LCE research. We examine the mechanical response of LCEs to stimuli and survey approaches for mechanical alignment, surface-enforced alignment, field-induced alignment and rheological alignment. The Review concludes with an over-the-horizon outlook discussing current challenges and emerging research opportunities.

The intrinsic properties of materials can be sensitive to external stimuli. This stimuli-responsiveness is a burgeoning area of research, in particular, for materials systems that emulate machines by transducing energy inputs into mechanical output[1]. More than 50 years ago, Pierre-Gilles de Gennes predicted that polymeric materials retaining liquid crystallinity would exhibit sizeable stimuli response comparable with the cooperative expansile–contractile response of a muscle fibre[2,3]. These compelling predictions motivated the synthesis of elastomeric polymer networks that retain liquid crystallinity[4–6]. These liquid crystalline elastomers (LCEs) are crosslinked polymer networks, whose stimuli response is associated with the disruption of order within the polymer network. Liquid crystallinity was initially preserved in local domains within the polymer networks; however, collectively, the domain orientations were random (that is, polydomain) (BOX 1). Subjecting these materials to processing (for example, mechanical deformation) during polymerization allowed the stabilization of a 'single-crystal' orientation (that is, monodomain) of the LCE[7]. The cooperative and reversible deformation enabled by the coordinated stimuli response of monodomain LCEs confirmed de Gennes' predictions.

The interplay of materials chemistry, processing, alignment and stimuli response remains a common theme in LCE research. Responses to deformation, both expected and peculiar (such as striping)[8], motivated theoretical research culminating in the detailed physical description of these materials[9,10]. Robust composition–structure–property correlations[11] have established the crucial importance of variables such as the degree of crosslinking, mesogen connectivity, domain orientation and phase. Two salient features of LCEs are particularly interesting from a materials science perspective, that is, large deformations (up to 400% strain) triggered by stimuli exposure (typically heat) and nonlinear deformation to mechanical load (often referred to as soft elasticity). The resurgence in LCE research is, in part, attributable to advances in materials chemistry and processing (for example, alignment) of LCEs that are broadly accessible to materials chemists, physicists and engineers[12,13], motivating the consideration of LCEs for applications in robotics[14], optics[15], health[16,17] and consumer goods[18] (FIG. 1).

In this Review, we discuss recent developments in LCE materials chemistry and materials processing, framed within a historical context. After introducing the mechanics and stimuli response of LCEs, we detail synthetic approaches to prepare LCEs grouped by how orientation is imparted to the material: mechanical alignment, surface-enforced alignment, field-assisted alignment and rheological alignment (3D printing). The Review concludes with an outlook to emerging research foci, unmet challenges and future opportunities.

Mechanics of liquid crystalline elastomers

LCEs are crosslinked polymer networks with polymer chains composed of a high concentration of rigid, rod-like segments based on interconnected aromatic or cyclohexyl rings. These rod-like molecular segments are

[1]*Department of Chemical and Biological Engineering, University of Colorado Boulder, Boulder, CO, USA.*

[2]*Materials Science & Engineering Program, University of Colorado Boulder, Boulder, CO, USA.*

✉*e-mail: timothy.j.white@colorado.edu*

https://doi.org/10.1038/s41578-021-00359-z

Box 1 | **Liquid crystalline elastomers**

Low-molar-mass LCs to LCEs:
Liquid crystals (LCs) of the calamitic type are thermotropic. Upon heating, they can transition from ordered (smectic, nematic) to disordered (isotropic) or ordered to less ordered (smectic to nematic). The rod-like mesogens in LCs are oriented along a director (**n**). The addition of reactive functional groups (such as acrylates, thiols or epoxides) onto the mesogens allows polymerization, resulting in crosslinked polymer networks that retain liquid crystallinity with mesogens within the main chain, side chain or as side-on pendants (see the figure, panel **a**).

Monodomain and polydomain:
The nematic phase is commonly retained in liquid crystalline elastomers (LCEs). The polydomain orientation of nematic LCEs is defined by local domains of nematic order (described by directors) that are macroscopically unaligned. When alignment is enforced, nematic LCEs can be described as monodomain. Monodomain LCEs have a common director that defines the orientation of the mesogens in the polymer network (see the figure, panel **b**).

Prolate, oblate and spherical:
The polymer chain configuration in a monodomain nematic LCE can take the form of a prolate or oblate ellipsoid. Oblate chain configurations, although rare, are typically realized in compositions with high side chain mesogen content. The isotropic configuration is spherical. The disruption of chain configuration by heat (or light) results in a dimensional change in the polymer chain configuration that produces the exceptional contraction and extension response in LCEs (see the figure, panel **c**).

Orientation:
Depending on the surface treatment and alignment method, mesogens within LCEs are anchored parallel (planar) or perpendicular (homeotropic) to the alignment surface. The planar or homeotropic orientation can perpetuate through the thickness of the film. Through-thickness variation can also be realized in twisted nematic or splay orientations between surfaces with different anchoring orientations (see the figure, panel **d**).

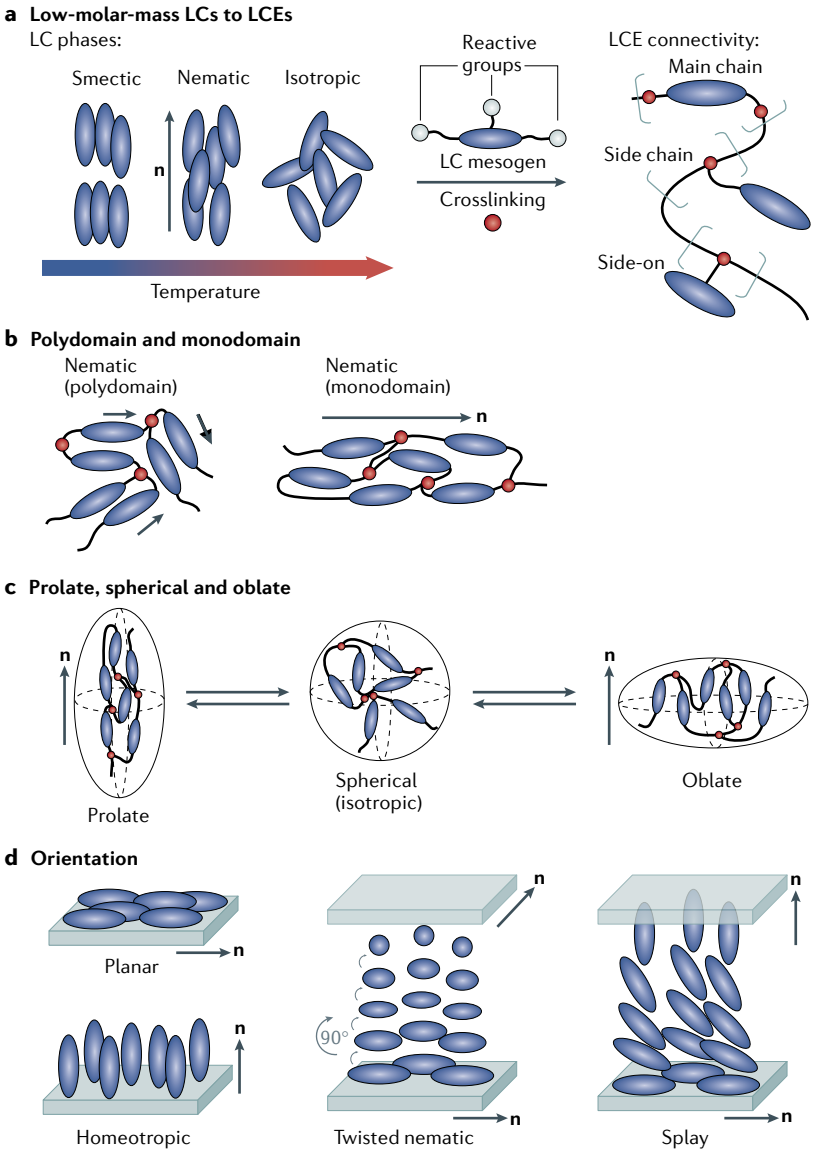

referred to as mesogens. Mesogens can be integrated into the main chain or the side chain of the polymer network (BOX 1). Liquid crystallinity is based on the intermolecular interactions between mesogens (π-stacking, dipole–dipole interactions). The intermolecular interactions of mesogens are retained within polymer networks and the mesogen–mesogen interactions can introduce local order. Notably, liquid crystallinity is retained in the polymer networks; however, the morphology is localized with micrometre-sized domains, unless the network is subject to an aligning field.

This Review is organized around four approaches to enforce global alignment to LCEs. Here, we define alignment as the application of an external force (mechanical, chemical, electromagnetic or rheological) to achieve collective orientation of the liquid crystalline segments in the polymer network. The orientation of liquid crystals (and LCEs) is directionally specified by an axial unit vector, that is, the director **n**. The relative degree of orientation of LCEs is defined by the order parameter *S*, which underpins the amplified stimuli-induced mechanical response and the distinctive nonlinear deformation of these materials to load.

Stimuli-induced mechanical response

The order retained in LCEs can be disrupted by exposure to stimuli. Embedded in the predictions of de Gennes[2], the decrease in orientational order with increasing temperature amplifies the relative magnitude of the material response, compared with conventional polymeric materials. The chemistry used to synthesize LCEs substantially influences the magnitude and rate of mechanical response; however, the fundamentals of the mechanics are largely agnostic to the composition of the material. The alignment of mesogens in the network (typically in the nematic phase) most commonly results in a prolate configuration of polymer chains within LCEs (BOX 1). In some cases, usually in LCE compositions prepared

with significant side chain mesogen concentrations, the polymer chain configuration is oblate (BOX 1). In general, the liquid crystalline segments within the polymer network are inherently thermotropic, akin to low-molar-mass liquid crystals[7]. Subjecting LCEs to heat disrupts the alignment of the mesogenic segments, causing the LCE to undergo an order–disorder transition. The local prolate (or oblate) polymer chain configuration transitions to a spherical configuration (BOX 1) upon heating. As in low-molar-mass liquid crystals, heat introduces kinetic energy to the molecules. Eventually, the LCE reaches a temperature at which the strength of the intermolecular forces is reduced by an increase in molecular motion and decrease in proximity, resulting in near-complete isotropy. This disruption of aligned liquid crystalline phases is the root cause of the comparatively large contractile strain evident in monodomain LCEs compared with conventional polymeric materials, and, further, imparts a directionality to the mechanical response. The largest dimensional change in the chain configuration of the polymer network is parallel to the director orientation of the liquid crystalline phase (BOX 1).

The magnitude of mechanical deformation depends on the orientation of the polymer network and the influence of the applied stimulus on order. LCEs can generally be considered crosslinked liquid crystalline polymers. However, the stimuli response of LCEs is different than in highly crosslinked and glassy polymers prepared by polymerization of high concentrations of multifunctional liquid crystalline monomers, referred to as liquid crystalline networks (LCNs) (FIG. 2). Within the broader classification of crosslinked liquid crystalline polymers, the magnitude of the stimuli response is coupled to an increase in molecular weight between crosslinks (MW_c), which corresponds to an increase in chain mobility in LCEs[19,20] (FIG. 2). Correspondingly, the stimuli response of LCNs is characterized by a limited decrease in order parameter and actuation of 5% strain or less. Comparatively, the mobility of polymer chains in LCEs is typified by a near-complete disruption of order and strain values from 40% to 400%.

The mechanical response of LCEs can also be induced by other stimuli. For example, additives can sensitize (nano)composite LCEs to indirectly convert optical[21], magnetic[22] or electrical[23,24] inputs into heat to induce a thermotropic response (FIG. 3a). Introducing photochromic constituents can impart isothermal phototropic phase behaviour to low-molar-mass liquid crystals[25,26]. For example, irradiating azobenzene-functionalized LCEs with ultraviolet light produces a photomechanical response[27] associated with the photoisomerization of azobenzene from the rod-shaped *trans* isomer to the bent-shaped *cis* isomer (FIG. 3b). The change in molecular shape disrupts the order within the network. Electromechanical effects have also been extensively examined in LCEs[28], and the compelling directional electromechanical effects are associated with the anisotropy in material stiffness, rather than with the disruption or reorientation of the mesogens within the polymer network[29–31] (FIG. 3c).

The directionality of the mechanical response of LCEs has long been limited to uniaxial deformation. However, the development of materials chemistries amenable to processing methods, such as surface-enforced alignment or 3D printing, have enabled the preparation of LCEs with spatial variation of the liquid crystal director orientation. Informed by predictions[32], reversible 3D shape transformations can be programmed during synthesis to transduce energy inputs into motion[14], actuation[33] and shape morphing[34]. As with the uniaxial deformation of LCEs[19], subjecting patterned LCE materials to a stimulus reversibly transforms the material from one shape (typically flat) to another (typically 3D) (BOX 2).

Stress-induced mechanical response

The molecular origins of the elastic deformation of elastomeric polymer networks are well understood[35]. The orientation of polymer chains within LCEs introduces differentiated mechanical deformation to load in that the stress–strain response to load is highly nonlinear. This was first observed in LCEs retaining polydomain orientation (that is, an LCE with local but not global alignment)[36]. The material maintains a linear relationship between applied stress and deformation until a threshold strain is reached, upon which a stress plateau is observed, often described as soft elasticity[37] (FIG. 4a). In this regime, small increases in applied stress can result in large changes in deformation (strain). Physically, the macroscopically unaligned domains in the material

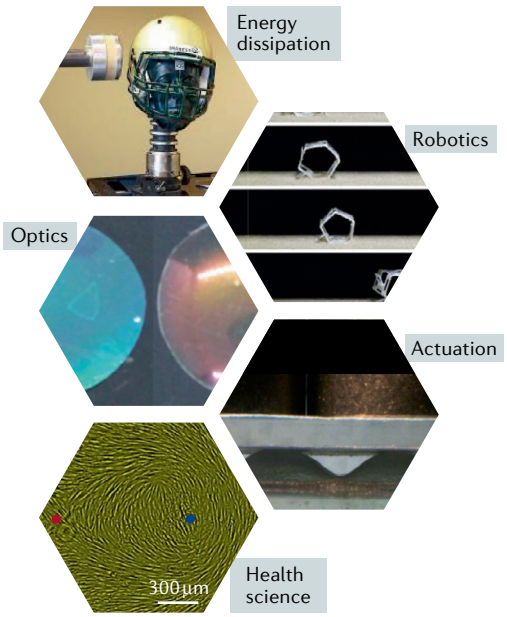

Fig. 1 | **Liquid crystalline elastomers as functional materials.** Liquid crystalline elastomers have been explored for functional use in energy dissipation of impact as a helmet lining, robotics, optics, actuation and health. Helmet lining image courtesy of University of Colorado Denver. Robot reprinted with permission from REF.[14], AAAS. Optics adapted with permission from REF.[15], Wiley. Actuation adapted from REF.[33], CC BY 4.0 (https://creativecommons.org/licenses/by/4.0/). Health science reprinted with permission of AAAS from REF.[17]. © The Authors, some rights reserved; exclusive licensee AAAS. Distributed under a CC BY-NC 4.0 License (http://creativecommons.org/licenses/by-nc/4.0/).

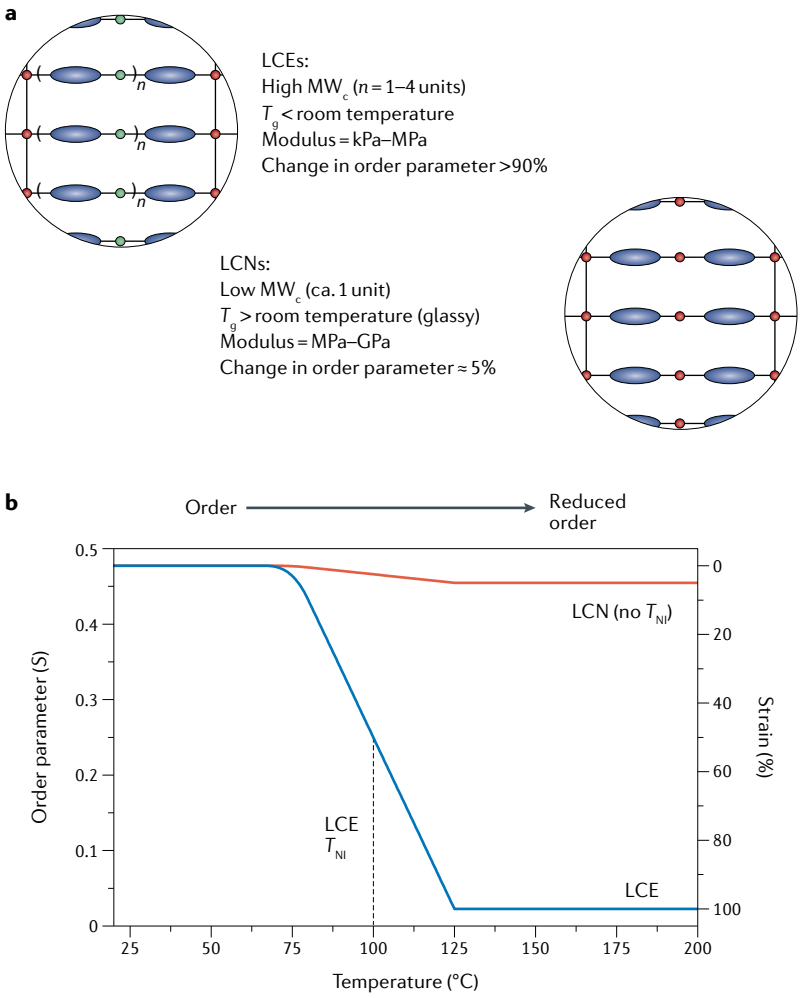

Fig. 2 | **Liquid crystalline polymer elastomers and networks. a** | The material properties that define liquid crystalline elastomers (LCEs) and liquid crystalline networks (LCNs) include molecular weight between crosslinks (MW_c), glass transition temperature (T_g) and modulus. The relative increase in polymer chain mobility allows LCEs to undergo a sizeable change in order. **b** | The relative increase in mobility increases the extent and rate at which the order parameter is affected by stimuli (here, temperature).

cooperatively orient along the loading direction. The reorientation of the director within these domains introduces nonlinearity to the stress–strain curve. Once the domains are collectively aligned to the loading axis, the material transitions from the soft elastic plateau and hardens to applied stress.

The mechanical deformation of aligned LCEs is also highly anisotropic[38] (FIG. 4b). When a monodomain (aligned) LCE is stretched parallel to the nematic director, the stress–strain curve is linear and described by classical rubber elasticity. However, when an LCE with monodomain orientation is loaded perpendicular to the nematic director, the material also exhibits soft elasticity and eventually transitions into a strain-hardening regime. An LCE in the homeotropic orientation (BOX 1) exhibits soft elasticity to loading in all axes (omnidirectional) orthogonal to the director, because mesogen alignment is orthogonal to the planar loading axis[39] (FIG. 4c).

The stress–strain response of LCEs can be considerably influenced by compositional variables, including the degree of crosslinking and the viscoelastic nature of the polymer backbone (for example, polyhydrocarbon or polysiloxane). The phase in which the polymer network is prepared (for example, 'genesis') can differentiate the mechanical response of LCEs in the polydomain orientation[40]. The distinct mechanical response of polydomain LCEs with isotropic or nematic genesis has been theoretically explained by the elastic memory associated with the formation of crosslinks in the polymer networks[41].

The cooperative mechanical alignment of liquid crystalline mesogens within polymers can also contribute to the mechanical response observed in amorphous elastomeric materials prepared with appreciable liquid crystalline content. Upon deformation, these materials exhibit mechanotropic phase transitions[42]; although amorphous (isotropic) upon polymerization, mechanical deformation of the material induces alignment of the liquid crystalline content, causing the formation of a nematic phase. The amorphous polymer network architecture enables rapid recovery compared with the elastic recovery of polydomain LCEs. This phenomena has been explored for photoelastic strain sensors[43] and is elastocaloric in nature.

The soft elastic and anisotropic deformation phenomena in LCEs can be exploited to spatially program local deformation to a global stress (load). Deformation in LCEs can be localized by patterning director orientation in monodomain nematic LCEs[44], homeotropic and planar regions in LCEs[39] and polydomain genesis in LCEs[45]. These strategies may, for example, be applied to ruggedize flexible electronic devices[46].

The sizeable stimuli-induced mechanical response and the nonlinear deformation of LCEs are associated with cooperative orientational changes in the polymer chains. The underlying physics of the stimuli response of LCEs are largely agnostic to the materials chemistry and materials processing. However, the approach to preparing these materials is paramount in dictating the magnitude and rate of response and determines the accessibility of materials preparation to non-chemists, as well as the potential for scale-up. The programmability of the stimuli response or deformation of LCEs depends on the compatibility of the materials chemistry with surface-enforced, field-assisted or rheological alignment.

Mechanical alignment of liquid crystalline elastomers

Mechanical alignment is the most common approach to preparing oriented LCEs, sometimes referred to as the 'Finkelmann method', and was first reported for the preparation of aligned polysiloxane LCEs[7]. Mechanical alignment of LCEs has since been extended to other chemistries[13]. In general, the mechanical alignment of LCEs is predicated on a two-step reaction: LCE compositions are first partially polymerized and subjected to load to bias (align) chain conformation along the loading axis, and then fully polymerized in the loaded state to arrest the aligned chain configuration (FIG. 5a,b).

Polysiloxanes by hydrosilylation

The original procedure to prepare aligned LCEs employed a two-step hydrosilylation reaction to form a polymer network composed of side chain mesogens[7] (FIG. 5c). This approach has been widely applied to prepare monodomain LCEs. The reaction occurs by hydrosilylation of liquid crystal monomers and crosslinkers with a linear polysiloxane in the presence of a platinum catalyst[7]. The initial reaction produces a weakly crosslinked polymer network as the vinyl liquid crystal monomers are initiated and incorporated into the developing polymer network. The preparation of LCEs by this reaction commonly exploits kinetic differences in the reactivity of two distinct crosslinkers. The faster-reacting polymerization of functional groups of one crosslinker forms a weakly crosslinked polymer network, which is then deformed under constant load to align the polymer chains. While under load, the polymerization reaction is restarted to complete the polymerization of the remainder of the slower-reacting crosslinker to form a robust, crosslinked polymer network. After the load is released, the LCE maintains the mechanically induced monodomain alignment. Cyclic siloxane can be copolymerized with multifunctional liquid crystalline monomers to prepare main chain LCEs by hydrosilylation[47].

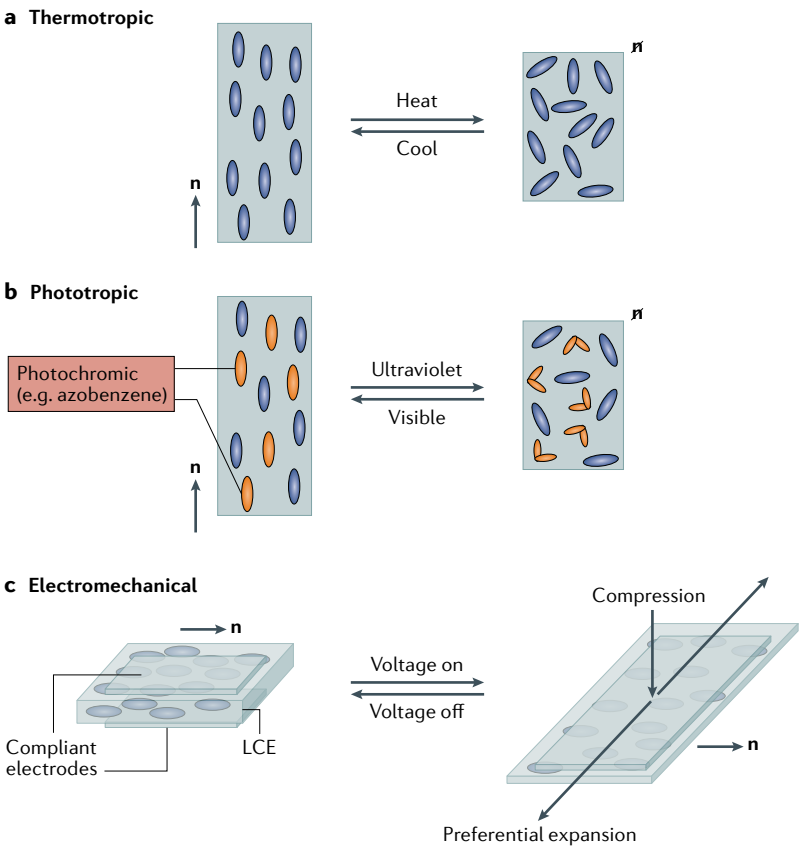

Fig. 3 | **Liquid crystalline elastomers as actuators. a** | Thermotropic disruption of order. In monodomain liquid crystalline elastomers (LCEs), heating transitions the material from a prolate to a spherical chain configuration. Macroscopically, this results in a directional strain parallel to the nematic director (accompanied by expansion in the other axes). **b** | Phototropic disruption of order. Similarly, light can also disrupt the order of LCEs composed of photochromic constituents, such as azobenzene. **c** | Electric field application does not readily induce changes in order or orientation in LCEs; however, electromechanical actuation can be observed in monodomain LCE encapsulated in flexible electrodes. Upon application of an electric field, the electrodes attract each other, generating Maxwell stress that deforms the material system preferentially along a single axis.

Chain extension of liquid crystalline monomers

Hydrosilylation reactions rely on non-commercially available materials and a nuanced, catalysed polymerization reaction. Alternatively, chain-extension reactions can be used to produce LCEs[12,13], including aza-Michael addition of diacrylate liquid crystalline monomers with primary amines[12] (FIG. 5d) and thiol-Michael addition of stoichiometrically excess diacrylate liquid crystalline monomers with thiols[13] (FIG. 5e). Both approaches are predicated on commercially available liquid crystalline monomers and photoinitiated polymerization[48]. Initially, the preparation of LCEs by chain extension focused on surface-enforced alignment; however, this chemistry is also amenable to mechanical alignment. Similar to LCEs based on polysiloxanes, LCEs prepared by thiol-Michael chain-extension reactions retain orientation upon removal of the load and undergo a two-step polymerization based on orthogonal initiation mechanisms. This chemistry has proven to be an accessible and increasingly popular approach to prepare LCEs. The formation of semi-crystalline domains in LCEs prepared with this reaction increase toughness and the relative force of actuation[49]. The reaction of acrylates and certain dithiols (FIG. 5f) include some chain extension, as will be described later; however, the formation of the polymer network is primarily related to a chain transfer.

Dynamic covalent chemistry

The incorporation of dynamic covalent chemistries (DCCs) into polymer networks for the preparation of covalent adaptable networks is an emerging area in chemical research[50]. Various DCC motifs have been incorporated into LCE compositions to enable mechanical alignment. Similar to mechanical alignment by two-step reactions (that is, hydrosilylation and chain extension), stimuli exposure can break and reform labile covalent bonds in LCEs subject to mechanical load. Upon removal of the stimulus while the material is subject to load, the material retains the mechanically programmed orientation. Initially, catalysed epoxide polymerization was used in LCEs[51]. Enabled by transesterification reactions, polydomain LCEs (formed in a one-step polymerization) are aligned by mechanical load at high temperatures and they retain this alignment. Transesterification[52–54], allyl sulfide[55] or polydisulfide[56] DCCs also allow mechanical alignment. Moreover, dynamic chemistries based on boronic esters[57], carbamates[58] and siloxanes[59] have been integrated into LCEs. In addition to enabling the mechanical alignment of LCEs, DCCs also extend potential functional opportunities, for example, shape memory, healing and reprocessing or recycling[50,60,61].

Surface-enforced alignment

Mechanical alignment of liquid crystalline polymer chains within LCEs is a straightforward approach to prepare LCEs with uniaxial orientation (FIG. 6a,b); however, this alignment method may not be easily scalable.

Furthermore, mechanical alignment is limited in the achievable complexity and resolution of spatial variation of the liquid crystalline orientation. Most large-area liquid crystalline displays are based on surface-enforced alignment. Surface-enforced alignment techniques rely on the interaction of liquid crystalline molecules with alignment coatings (that is, command surfaces) that enforce orientation by topological entrapment[62] to anchor liquid crystalline molecules near these surfaces (FIG. 6c). The lowest energy state f_0 for an aligned nematic liquid crystal occurs when there is no deviation from the director **n**. For imperfectly aligned liquid crystals, or those with bend (K_1), twist (K_2) and splay (K_3) contributions to the free energy through the bulk, the distortions contribute additional elastic energy terms according to the Frank free elastic energy density[63]:

$$f_d = \frac{1}{2}K_1\left(\vec{\nabla}\cdot\vec{n}\right)^2 + \frac{1}{2}K_2\left(\vec{n}\cdot\left(\vec{\nabla}\times\vec{n}\right)\right)^2 + \frac{1}{2}K_3\left(\vec{n}\times\left(\vec{\nabla}\times\vec{n}\right)\right)^2 \quad (1)$$

Box 2 | **Patterned response in liquid crystalline elastomers**

The director orientation of liquid crystalline elastomers (LCEs) can be spatially patterned by surface-enforced alignment, rheological alignment or field-assisted alignment. One common pattern is described as a +1 topological defect, in which the nematic director forms concentric circles around a point. When the order of the material is disrupted by heat or light, the local variation of strain is orthogonal to the nematic director and results in the material transitioning from a flat state to a cone. Relatedly, application of an electric field to an LCE patterned with this director profile also forms a cone but does so due to spatial variation in modulus, which defines the local direction and magnitude of deformation.

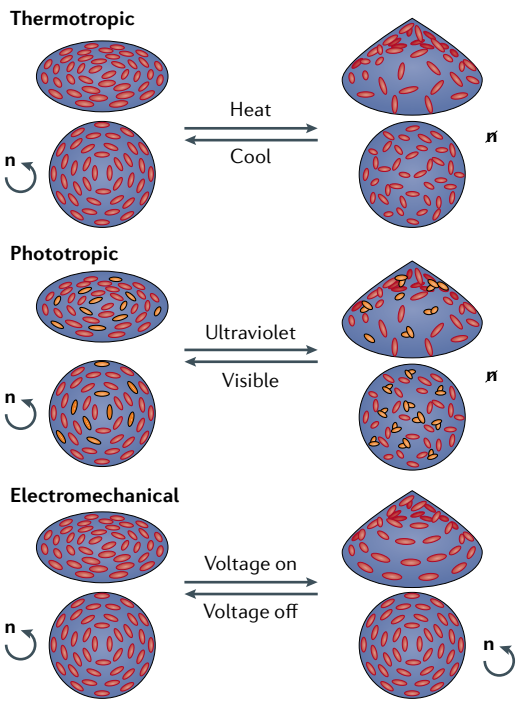

If there is no pretilt and the director field $\vec{n} = (\cos\varphi, \sin\varphi, 0)$ is purely azimuthal in orientation, for the in-plane angle $\varphi(x, y, z)$, the elastic coefficients K_i are approximately equal and f_d reduces to:

$$f_d = \frac{1}{2}K(\nabla\varphi)^2 \quad (2)$$

For liquid crystal molecules adjacent to command surfaces, the free surface energy is distinct from the bulk and originates from isotropic (surface-tension-based) and anisotropic (anchoring energy) components. Therefore, the total energy of a surface-aligned cell includes contributions from the Frank free elastic energy density and the surface energies of the alignment cell. The presence of a magnetic or electric field also contributes to the total free energy of the system.

By enforcing alignment at these interfaces, the thermodynamic preference of liquid crystals to align with one another extends across distances of up to ~50 µm (REF.[33]). The interaction length is defined by the strength of intermolecular interaction amongst the mesogens and the chemical affinity of the liquid crystal media and the alignment material. The interplay of these considerations is nontrivial, with orientational relaxation effects present across the volume of the cell[63]. Surface-enforced alignment techniques are uniquely amenable to preparing LCEs with through-thickness variation in the orientation of the director (twisted nematic[64] or splay orientation[64,65]) (BOX 1) or to preparing LCEs with spatial variation in orientation.

Aza-Michael addition of liquid crystalline monomers

The polymerization of liquid crystalline monomers to form moderately crosslinked and glassy LCNs has long been known to be conducive to surface-enforced alignment[66]. Elastomeric LCNs (that is, LCEs) show sizeable changes in order in response to stimuli, owing to polymer network mobility afforded by the large MW_c (REF.[20]) (FIG. 2). Of note, surface-enforced alignment of LCEs prepared by hydrosilylation, thiol-Michael chain extension or dynamic covalent chemistry has not yet been realized.

A 'one-pot' preparation of 'voxelated' LCEs by surface-enforced alignment has been reported within the confines of a liquid crystal alignment cell[12]. Here, the LCEs were prepared by subjecting classical liquid crystal diacrylate monomers to chain extension by aza-Michael addition with an amine. This reaction is amenable to surface alignment because the reaction originates from the liquid crystalline phase with a low starting viscosity and the kinetics of the oligomerization reaction are slow. The concentration of the primary amine to the diacrylate liquid crystalline monomer can be varied to adjust the MW_c while retaining liquid crystalline character. Variation of the MW_c dictates the resulting magnitude and rate of the thermomechanical response[20]. Anecdotally, if the chain-extension reaction proceeds too quickly, the mesogens do not strongly retain alignment, resulting in poorly aligned LCEs. Through the inclusion of a photoinitiator, the acrylate-endcapped oligomers can be subsequently photopolymerized to prepare a polymer network, all within the alignment cell. The composition of the amine pendant groups can affect the thermomechanical

response of LCEs prepared from the aza-Michael addition reaction[67,68]. This materials chemistry has also been employed to prepare azobenzene-functionalized LCEs, including a diacrylate azobenzene comonomer[69].

Photopolymerization of acrylate and thiol-ene compositions

Monofunctional and difunctional liquid crystalline monomers can be copolymerized to increase the MW_c in LCNs[70]. These LCNs are mainly composed of side chain mesogens and maintain glass transition temperatures above room temperature[70]. Accordingly, despite the reduction in crosslink density, the magnitude of their mechanical response is limited compared with LCEs, owing to the limited mobility of (typically) polyacrylate networks and the reliance on side chain mesogens.

The aza-Michael addition reaction results in LCEs with main chain mesogens. Using appropriate amine concentrations, the molecular weight of the oligomeric precursors can be tailored to suppress the glass transition temperature to well below room temperature. LCEs with low crosslink density can also be prepared by direct photopolymerization of mixtures formulated from liquid crystalline monomers[71,72], which requires minutes to synthesize LCEs. For example, a thiol-ene reaction of a dithiol monomer and liquid crystalline monomer with diallyl ether functional groups has been used to prepare LCEs[71]. Here, the allyl ether moieties do not readily homopolymerize[73], and, accordingly, the reaction proceeds primarily by step-growth polymerization. A diacrylate liquid crystalline included in the formulation contributes as a crosslinker. This LCE composition is amenable to surface-enforced alignment and has a thermomechanical response of 160% strain[20]. Alternatively, monofunctional and difunctional thiols can be used as chain transfer agents to prepare LCEs[72] (FIG. 5f). Although the chain configuration of the polymer network is not fully understood, similar polymerizations have resulted in hyperbranched polymer networks[74]. Here, conventional diacrylate liquid crystalline monomers were mixed with thiols that could either not participate in chain-extension reactions (monofunctional thiols) or that are known chain transfer agents. Photoinitiated polymerization then results in an LCE with a low glass transition temperature, actuation strain of up to 50% and high optical quality (<0.25% haze). This LCE composition is based on low-molar-mass liquid crystalline monomers, and is, thus, amenable to surface-enforced alignment. The same chemistry can be applied to layer LCEs, which achieve a work density of more than 20 J kg^{-1} (REF.[33]), or to realize large-scale thermochromism (thermally driven colour change) in LCEs that retain the cholesteric phase[15]. However, likely owing to the complicated network architecture, the mechanical deformation and elastic response[75] of these materials exhibit strain-dependent recovery to load.

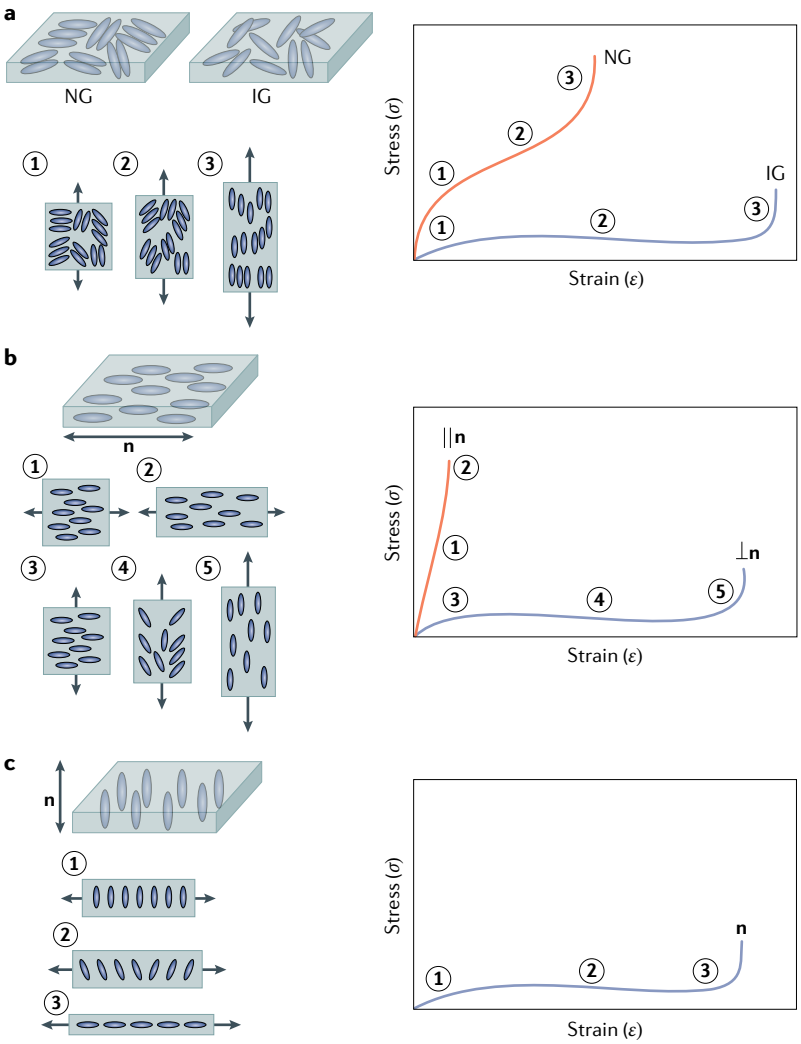

Fig. 4 | **Nonlinear deformation of liquid crystalline elastomers to load.** The deformation of liquid crystalline elastomers (LCEs) to load is distinct from conventional elastomeric materials and depends on domain orientation. **a** | The local orientation of the liquid crystalline mesogens in polydomain LCEs align to the loading axis. The mechanical response of polydomain LCEs is dependent on the genesis of the material. The deformation of isotropic genesis (IG) and nematic genesis (NG) polydomain LCEs is illustrated. The deformation of polydomain LCEs is classified by an initial linear deformation (phase 1), a soft elastic region (phase 2) and a strain-hardening regime (phase 3). **b** | The mechanical deformation of monodomain LCEs is illustrated under load parallel and perpendicular to the nematic director (**n**). When loaded parallel to the nematic director, monodomain LCEs exhibit classical deformation (phases 1, 2). When monodomain LCEs are loaded perpendicular to nematic director, the mesogens within the polymer network reorient along the loading axis, resulting in an initial linear deformation (phase 3), a soft elastic plateau (phase 4) and a strain-hardening regime (phase 5). **c** | The mechanical response of homeotropic LCEs, in which the nematic director is normal to the LCE surface. Reorientation towards direction of applied stress results in soft elasticity along all loading axes (phases 1–3).

Spatial variation in orientation

Photoalignment. An important subclass of surface-enforced alignment is based on photoresponsive command surfaces (that is, photoalignment). Initially developed by the display industry to reduce physical contact with large, flat-panel substrates[76], a range of alignment materials have been explored, including azobenzene dyes, cinnamates and so-called 'linearly polarized polymers'[77]. In general, these compositions are cast onto a surface (typically glass). In the case of azobenzene, irradiation with linearly polarized blue light induces stochastic alignment of the dye molecules by the Weigert effect[77,78]. In some liquid crystal mixtures, the alignment of the dye molecules is translated to the liquid

crystal. Owing to spatiotemporal control of light irradiation, most notably linear polarization, complex patterns can be imprinted into photoalignment materials[79,80]. Photoalignment has been used to prepare LCEs with complex director profiles, with all three chemistries discussed in the previous section, including imprinting of images, director profiles and arrays of director fields[12,71,72]. Photoalignment is a high-resolution and rapid approach to 'voxelate' the local alignment within LCEs. The resolution scales with sample thickness[63].

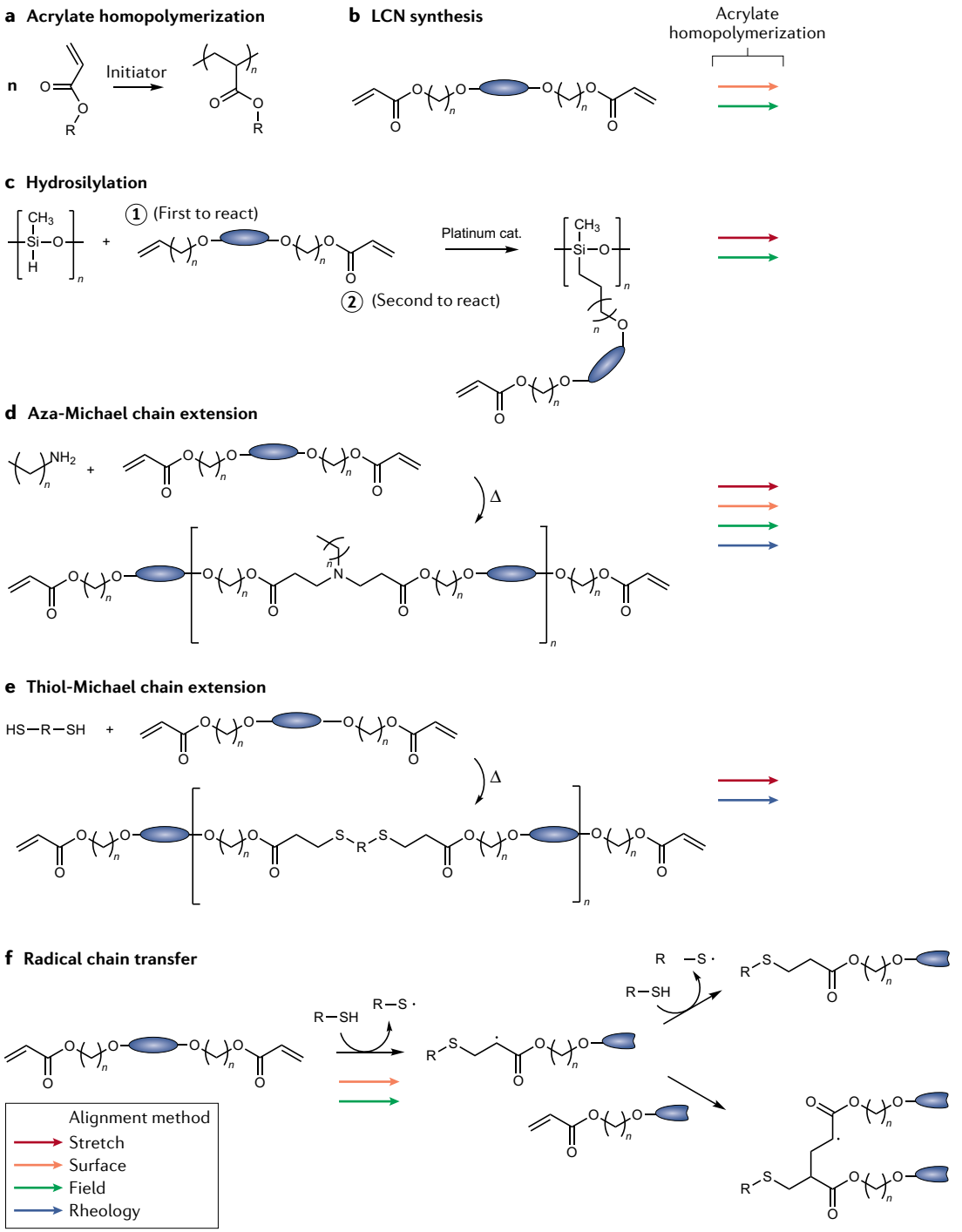

Fig. 5 | **Synthetic approaches for the preparation of crosslinked liquid crystalline polymers.** Liquid crystalline networks (LCNs) are commonly based on a photoinitiated acrylate homopolymerization (panel **a**) to prepare LCNs amenable to surface or field alignment (panel **b**). Aligned liquid crystalline elastomers are prepared by the two-step 'Finkelmann method' (panel **c**), comprising a platinum-catalysed hydrosilylation, followed by a photoinitiated radical crosslinking polymerization (stretch and field alignment), aza-Michael oligomerization and successive photo-crosslinking (stretch, surface, field and rheological alignment) (panel **d**), thiol-Michael chain extension and subsequent photopolymerization of residual groups (stretch and rheological alignment) (panel **e**), and a radical chain transfer reaction (surface and field alignment) (panel **f**).

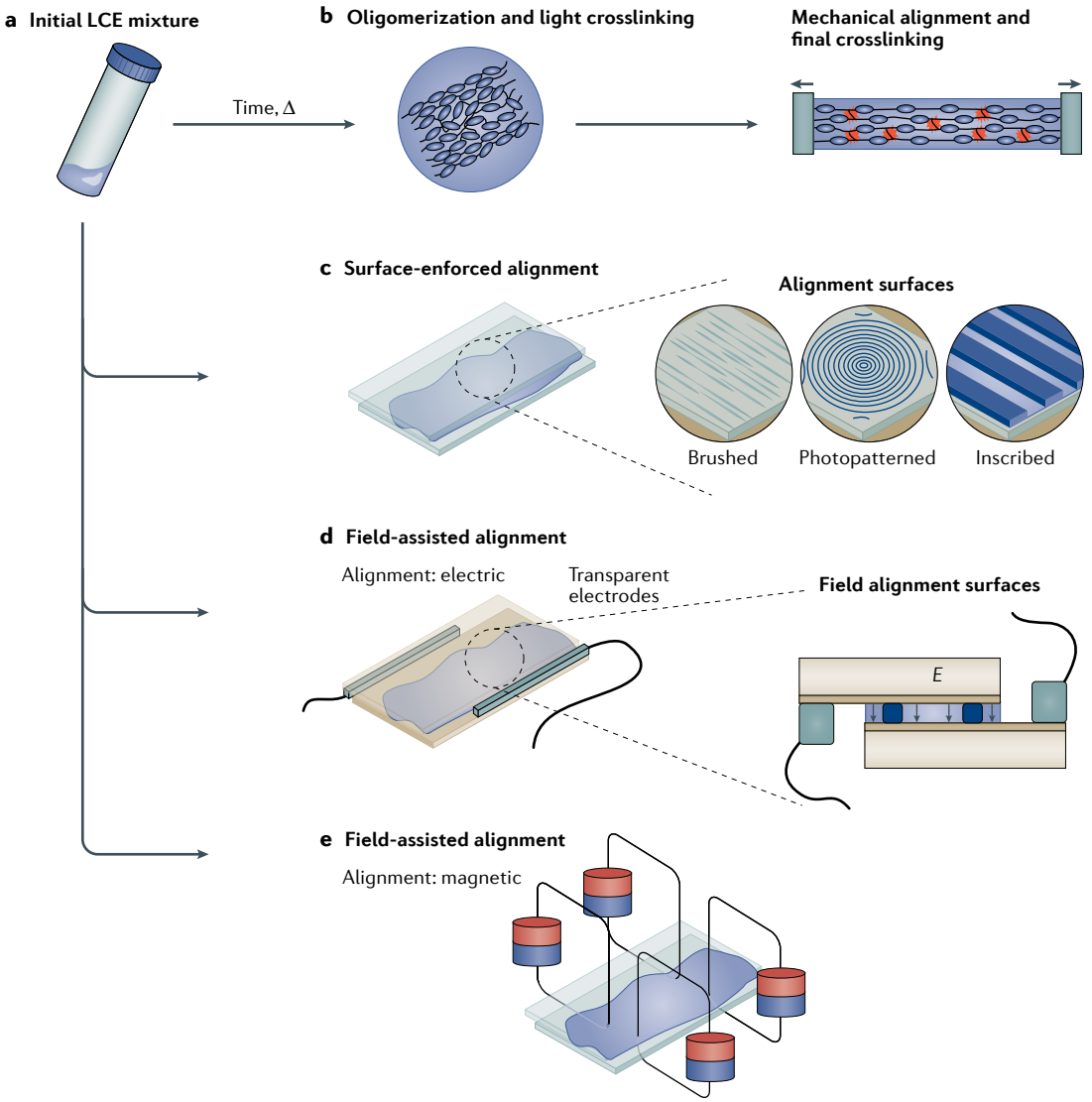

Fig. 6 | **Alignment of liquid crystalline elastomers. a** | Liquid crystalline elastomer (LCE) mixtures can be aligned through mechanical alignment of oligomerized or partially polymerized networks induced by a mechanical force (panel **b**). **c** | Some LCE compositions are amenable to surface-enforced alignment by brushing, photopatterning or inscribing to guide mesogen orientation. **d** | Application of an electric field to cells with uniform or patterned electrodes align the liquid crystalline monomers to the field orientation. Indium-tin-oxide-coated glass and electrodes are attached to the cell to enable field application across the cell. **e** | The orientation of liquid crystalline networks and LCEs can be enforced by a magnetic field.

Optical methods to introduce complex director profiles include laser rastering[12], projection from a spatial light modulator[63] and plasmonic masks[81].

Localized surface rubbing. Another approach to vary the local orientation by surface-enforced alignment is surface rubbing. Most liquid crystalline displays are prepared with alignment coatings subjected to macroscopic surface rubbing, which introduces microscopic grooves into the material[62]. The liquid crystal alignment direction **n** follows the orientation of these grooves. Thus, locally varying the orientation of the rubbing direction on an alignment substrate can vary the orientation of the liquid crystalline director. Localized surface rubbing has not been widely explored as an approach to introduce alignment patterns within LCEs. Conceivably, a master prepared by rubbing (for example, by atomic force microscopy)[82] could be replicated with moulding and scaled to prepare LCEs with precise topological director profiles.

Lithographic patterns. A hybrid of photoalignment and localized surface rubbing has been used to enforce spatial variation in the alignment of LCEs. By leveraging photolithographic methods, light can be used to prepare topographically patterned substrates, which then serve to enforce uniaxial or complex alignment onto LCEs[83,84]. The process is predicated on patterning a negative photoresist layer (such as SU8), which is selectively removed by irradiation with a resolution limit set by the wavelength of the light[85]. For example, an SU8 master has

been replicated with a polydimethylsiloxane template. Complex geometries, such as microchannel or micropillar LCE arrays, with precise shape change and actuation have been realized[83,86]. This approach is not exclusive to photolithography, and could be extended to e-beam lithography. In addition to enforcing alignment a priori, imprint lithography can also be used to adjust the form of an already prepared LCE. For example, an LCE/covalent adaptable network was patterned with imprint lithography to prepare self-healing micropillars[56].

Field-assisted alignment

Liquid crystalline molecules align to electric and magnetic fields. The electro-optic response of liquid crystals is prevalent in daily life in the implementation of these materials in displays. Light is modulated by adjusting the strength of the applied electric field, which orients the liquid crystals for a given pixel. As with displays, the basis of field-assisted alignment is the anisotropy of the dielectric constant or diamagnetic susceptibility of liquid crystals. Although electrical reorientation of mesogens in polymerized LCEs is technically achievable, it requires exceptionally high voltages above the dielectric breakdown voltage of many compositions. Thus, field-assisted alignment to prepare LCNs or LCEs requires materials chemistries that originate from low-viscosity, low-molar-mass components.

Electric field

A prerequisite in the molecular design of liquid crystalline materials is the incorporation of polar functional groups (for example, esters, nitriles or halogens). Many common display modes are based on liquid crystalline compositions with positive dielectric anisotropy. The dielectric anisotropy of a liquid crystal is positive if the dielectric constant along the longitudinal axis of the molecule is greater than the value for the lateral axis, inducing mesogen alignment parallel to the applied electric field. However, to our knowledge, all commercially available diacrylate liquid crystalline monomers have a negative dielectric anisotropy[87]; that is, the dielectric constant is greater along the lateral axis of the molecule, inducing mesogen alignment perpendicular to the applied electric field. Accordingly, application of an electric field across parallel-plate electrodes in a conventional liquid crystal alignment cell strongly enforces planar alignment to these compositions (FIG. 6d). Monofunctional liquid crystalline monomers have been synthesized with polar head groups (such as a nitrile)[6] and maintain a positive dielectric anisotropy. Mixing these monoacrylate liquid crystal monomers with diacrylate liquid crystal monomers can change the average dielectric anisotropy of the mixture (from negative to positive), to allow electric field alignment of these materials into the homeotropic orientation, which can be retained upon polymerization[88].

Electric-field-assisted alignment has been sparingly used to prepare LCEs in planar and homeotropic orientations[15,89–93]. Similar to photoalignment, electrode patterning has been explored to spatially vary the orientation (for example, planar or homeotropic)[88] or even to distort the director profile across the material cross section in LCNs[90]. In regions of the material subjected to an electric field, a threshold field strength E_c must be surpassed to disrupt the static field-off director field according to the relationship,

$$E_c = \frac{\pi}{d}\sqrt{\frac{K_i}{\varepsilon_0 \Delta\varepsilon}} \tag{3}$$

where K_i is the Frank elastic coefficient, ε_0 is the permittivity of free space, $\Delta\varepsilon = \varepsilon_{||} - \varepsilon_{\perp}$ is the anisotropy of the dielectric susceptibility and d is the cell thickness[94,95]. The reorientation of liquid crystal molecules to strong external fields is known as the Fréedericksz transition.

An electric field can also be used to enhance the orientation of liquid crystals in compositions already subject to surface-enforced alignment[15]. A challenge in using electric fields to assist in the preparation of patterned LCEs is the need for reaction chemistries that either exhibit surface-enforced planar alignment and positive dielectric anisotropy or homeotropic surface-enforced alignment and negative dielectric anisotropy, such that application of an electric field selectively reorients LCE precursors. Surface-enforced alignment has been demonstrated for the preparation of LCNs[91]; however, the preparation of LCEs that are locally readdressed with electric fields (for example, by electrode patterning) to orient to the homeotropic state requires the incorporation of monofunctional liquid crystalline monomers with polar head groups (and, subsequently, positive dielectric anisotropy). This inevitably results in LCEs with a high concentration of side chain mesogens or, in the case of chain-extension reactions, branches from the incorporation of mesogen-terminated oligomers.

Magnetic field

Liquid crystals can also be aligned by a magnetic field, analogously to the association of electric field alignment and dielectric anisotropy of susceptible liquid crystalline materials. Aromatics[96] have a high magnetic susceptibility perpendicular to the plane of the ring. Thus, the prevalence and orientation of these rings in liquid crystalline materials are the primary sources of the large and anisotropic diamagnetic susceptibility of these materials. Owing to their aromatic character, most liquid crystals exhibit positive diamagnetic anisotropy and orient their long axis parallel to the applied magnetic field. Liquid crystalline materials prepared with cyclohexyl rings maintain low (and often negative) values of diamagnetic anisotropy, which results in the long axis of these molecules aligning perpendicularly[97]. Magnetic fields have been extensively used to assist the alignment of LCEs[98]. Adjusting the orientation of the magnetic field by concurrent exposure from multiple sources can locally prescribe complexity of the director in LCEs[99] (FIG. 6e).

The magnetic field extension of the Fréedericksz transition is analogous to that for electric fields, described by the relationship,

$$H_c = \frac{\pi}{d}\sqrt{\frac{K_i}{\mu_0 \chi_a}} \tag{4}$$

where H_c is the magnetic field threshold, d is the cell thickness, K_i is the Frank elastic coefficient, μ_0 is the free space permittivity and χ_a is the diamagnetic susceptibility. Here, the threshold magnetic field H_c required to induce alignment is inversely related to the anisotropy of the diamagnetic susceptibility χ_a. The relative sensitivity and amenability of a particular LCE composition to magnetic field alignment is primarily dictated by the diamagnetic susceptibility, but is also influenced by other considerations, such as surface anchoring. The magnetic field emanating from a strong permanent magnet will generally suffice in altering the alignment of aromatic-cored mesogens. Increasing the magnetic field strength above a threshold value does not further improve the degree of alignment[99]. A key distinction, compared with purely surface-enforced alignment methods, is that magnetic field alignment acts on the collective volume of the liquid crystalline composition. This allows for uniform orientational control throughout the entire thickness, which can be advantageous for preparing thick samples (>50 μm), as well as thin samples. Magnetic field alignment in LCEs has been applied to prepare uniaxial[100,101], homeotropic[86,102] and radial director patterns[99].

Spatial patterns in LCNs have also been prepared by digital light processing (DLP), enabled by the use of a magnetic field[103]. During printing, the fields emanating from permanent magnets, which circumferentially surround a polymer resin bath, can be adjusted to programmatically exceed the threshold magnetic field H_c needed for liquid crystalline alignment. Individual layers and voxels can be addressed with a defined magnetically assisted orientation, and the resulting director profile is entrapped by ultraviolet light, curing the LCE resin in the build layer. Although initially used to prepare moderately crosslinked LCNs, this fabrication strategy can also be employed for complex LCE actuators and mechanical metamaterials. However, DLP and other additive techniques (such as inkjet and direct laser writing) have been limited to larger LCEs, owing to the constraints of alignment. For example, microstructured light-responsive cilia have been selectively patterned with inkjet, but this requires deposition of the monomer precursors as thin films onto an alignment surface[104]. Similarly, direct laser writing can be used to fabricate microstructured actuators, such as light-responsive microwalkers[105,106] and other devices[107], as long as they are prepared in contact with a surface-aligned substrate. To leverage the diversity of 3D printing methods to prepare LCEs will require wider integration of magnetically assisted alignment or the development of other strategies to achieve volumetric alignment.

Rheological alignment

Rheological alignment of liquid crystals is a well-known approach to introduce and direct orientation[108,109]. Here, we focus on the exploitation of rheological orientation of liquid crystals in flow for the 3D printing of LCEs. Additive printing techniques based on the flow of materials include direct ink writing (DIW)[110,111], fused deposition modelling and electrohydrodynamic jet[112]. Amongst these approaches, DIW has proven to be best suited to prepare aligned LCEs by printing thus far.

The flow of colloidal and organic DIW ink gels is shear thinning and can be described by the Herschel–Bulkley model:

$$\tau = \tau_y + k\dot{\gamma}^m \quad (5)$$

where k is the consistency coefficient (or viscosity parameter), m is the flow behaviour index ($m<1$ for shear thinning), τ_y is the yield stress, τ is the stress and $\dot{\gamma}$ is the shear rate[113]. Extruded through a cylindrical printhead, and depending on velocity gradients across the cross section of the printhead radius and ink stability, the LCE inks exhibit a three-zone shear rate (velocity) profile that includes an unyielded gel core (constant velocity), a yielded fluid shell layer undergoing laminar flow and a thin slip layer[114] (FIG. 7a,b).

In DIW, the liquid crystalline content is typically forced to align, owing to both shear and extensional stresses during extrusion through a printhead. Liquid crystalline shear flow, well described by the Ericksen–Leslie continuum theory of liquid crystals[115], can be specified by a series of constants characterizing torque experienced during shear flow; here, uniform flow occurs when shear-induced torque is vanishing along the plane of shear. A physical explanation for liquid crystal flow alignment dynamics in terms of a continuum model relates the direction of flow and the plane of vanishing torque to the ratio of major and minor axes in the liquid crystal mesogens, as well as to the overall viscosity of the matrix[116]. In this theory, liquid crystal flow dynamics are deconstructed into a function of velocity and director vectors[117,118]. In situ polarization rheology has further elucidated the dynamics of anisotropic alignment in concentrated solutions of cellulose nanocrystals, in particular, the dynamics of anisotropic particles during extensional alignment[119]. Eliminating the contributions of the extensional alignment geometry during capillary flow identifies a critical radius inside which plug flow (and not shear flow) occurs, resulting in only a thin (25-μm) shell of aligned material in the extruded filament. Conversely, with an extended tapered tip geometry and a long residence time of cellulose nanocrystals under shear, the contributions from extensional alignment — which are also expected from the high linear oligomer content in oligomerized liquid crystalline inks — induce more alignment within the filament. Ultimately, contributions of shear and extensional flow to materials printed with DIW are dictated by the relative contributions of velocity and director vectors[117], as well as viscosity, residence time and tip geometry.

Rheological alignment of oligomers prepared by chain-extension reactions

DIW for LCE printing was first demonstrated with printable inks prepared by the aza-Michael oligomerization reaction[120] (FIG. 7c). Studies using oligomeric precursors subjected to the shear and extensional flow conditions of 'hot' DIW (85 °C) confirmed that acrylate-terminated oligomers readily align to flow direction upon extrusion. DIW oligomers retain a high degree of liquid crystalline order in their director profiles (described by their order parameter), with immediate photopolymerization

following extrusion. It was also shown that Newtonian flow behaviours in inks prepared by aza-Michael reactions at higher temperatures (nearing the isotropic state) transition into shear-thinning rheological behaviour at lower temperatures, which improves the quality of the printed materials[121]. Informed by these rheological

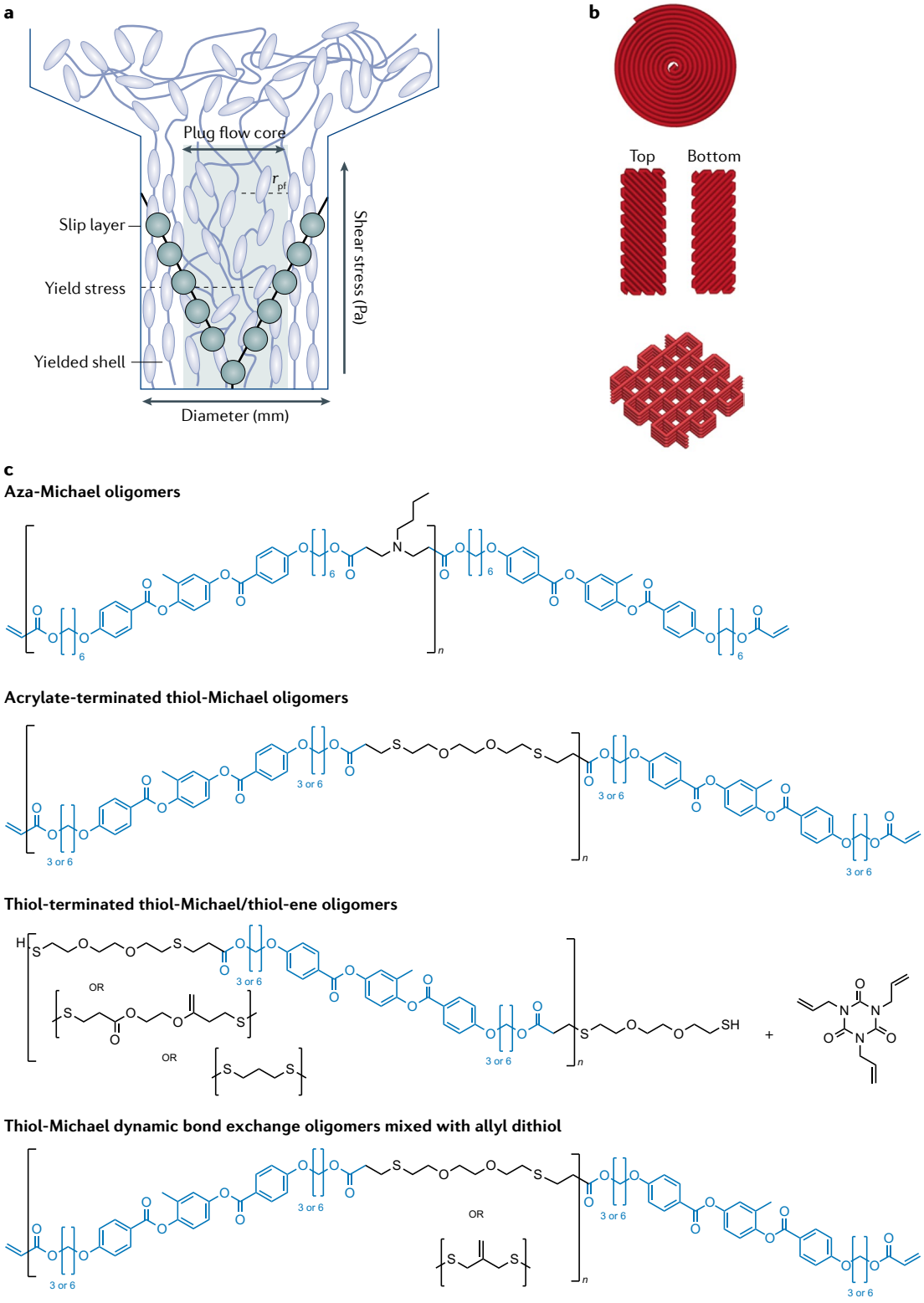

Fig. 7 | **Direct ink writing of liquid crystalline elastomers. a** | The printhead diameter directs cross-sectional flow dynamics of extruded formulations. **b** | The print paths can be used to prepare patterned liquid crystalline elastomer films. **c** | Liquid crystalline elastomer ink compositions amenable to rheological alignment include aza-Michael oligomers, acrylate-terminated thiol-Michael oligomers, thiol-terminated thiol-Michael/thiol-ene oligomers and thiol-Michael dynamic bond exchange oligomers mixed with allyl dithiol. Panel **b** reprinted with permission from REF.[120], American Chemical Society.

measurements, orientation parameters up to 0.40 have been retained in printed LCEs, rivalling those measured in surface-enforced alignment (0.45). In addition to the effect of temperature on the orientation of printed LCEs, the order parameter correlates with other variables, including print speed and print diameter.

Chain-extension reactions have also been explored using the thiol-Michael addition reaction. For example, excess diacrylate liquid crystalline monomer was mixed with a dithiol chain extender and a base catalyst to drive the formation of chain-extended linear acrylate-terminated oligomers within the ink precursor matrix[122] (FIG. 7b). This oligomerization yielded a room-temperature-printable ink at print speeds between 5 and 10 mm s^{-1}, which requires immediate photopolymerization to lock in the orientation. Actuation strains within the fully cured DIW filaments (associated with the printhead diameter) decreased from 48% to 34%, with an increase in filament diameter, attributable to reduced alignment. This effect is consistent with the known relationship between nozzle radius, volumetric flow rate and the shear rate experienced by the flowing ink in DIW, which can be estimated as:

$$\dot{\gamma}_{max} = \left(\frac{3+b}{4}\right)\frac{4\dot{Q}}{\pi R^3} \quad (6)$$

where $\dot{Q}$ is the volumetric flow rate, R is the nozzle radius and b is the inverse of the flow behaviour index (the inverse of m in Eq. 5)[111,123].

Other ink compositions have been explored that further extend the molecular engineering of chain-extension reactions[124]. For example, the thiol chain extender and diacrylate liquid crystalline monomer content can be varied in the presence of a tertiary amine catalyst to produce high-weight-fraction linear chains within the ink precursor matrix (FIG. 7b). In contrast to ambient thiol-Michael inks with acrylate-terminated linear chain content, the stoichiometry in these formulations leads to thiol end groups on the growing oligomer chains. Unreacted thiols can be fully cured after DIW extrusion by the incorporation of allyl 'ene' monomers, which do not homopolymerize but readily react with thiyl radicals. Furthermore, a printed LCE was prepared using dynamic covalent chemistry (allyl sulfide bonds). Light-activated dynamic bond exchange (FIG. 7c) then allows modification of the polymer network in printed LCEs[125]. Conventional actuation of LCE devices requires constant energy to sustain shape change and force output. Here, the shape of the printed LCE can be retained after removal of the stimulus, enabled by photoinduced retention (or release) of thermally generated stress.

Of note, the specific work and actuation strain for printed LCEs scale with aligned thickness. Accordingly, patterned LCEs prepared by 3D printing (DIW) can be used to prepare material actuators. Owing to rheological alignment, the local mesogen director is dictated by the printing path, which can be exploited to prepare topological defects and snap-through instabilities[120,121] (FIG. 7b). For example, DIW LCE cone arrays within radio-frequency identification tag devices can be applied for passive and cost-effective temperature sensing[126,127]. Moreover, the exceptional work outputs, compliance and processability of 3D-printed LCEs are particularly appealing for functional use in soft robotics[14]. For example, by combining elastomeric substrates and conductive ink traces, electrothermal actuation enables soft grippers to lift ping-pong balls[122].

Outlook

Since de Gennes' predictions, LCEs have evolved from an abstract concept to a popular and increasingly examined class of stimuli-responsive materials. The introduction of new materials chemistries has further enabled the preparation of compositions that are widely adoptable and amenable to processing techniques, which allow the 'programming' of the mechanical response of LCEs and, thus, functional applications. Future research of LCEs will continue to involve investigations of materials chemistries, actinic energy inputs and the exploration of more advanced functional implementations.

Materials chemistry of liquid crystal elastomers

Advances in the materials chemistry of LCEs have made them amenable to processing. However, fundamental investigations remain limited, in particular, on the molecular weight dependence of oligomers subject to surface-enforced alignment, the use of patterned electric fields to pattern LCE orientation and advanced rheological studies of printable inks. In addition, more scalable and robust chemistries need to be explored. Indeed, neither popular approach to preparing LCEs by chain-extension reactions is optimal. The preparation of oligomers at appropriate kinetics by aza-Michael addition to retain surface-enforced alignment[12] is slow, typically occurring over timescales of 12–24 h. However, enforcing alignment by directed self-assembly is highly scalable, evident in the well-established manufacture of liquid crystalline devices. Conversely, the preparation of oligomers by thiol-Michael addition reactions are comparatively fast[13] and have become widely adopted. However, owing to the rapid development of high-molecular-weight starting materials, these reactions are not yet amenable to surface-enforced alignment. Uniaxial alignment of LCEs is useful in generating linear actuators; however, many of the most compelling functional opportunities for LCEs seem to originate from the unique opportunity to prepare monolithic materials systems that have been designed from the bottom up to achieve spatially distinguished responses. The use of radical chain transfer can circumvent some of these limitations and makes LCEs amenable to surface-enforced alignment; however, the resulting polymer network morphologies are not well understood[72,128] and can exhibit hysteresis[75].

3D printing of oligomeric inks by DIW[14,120–122,124,125,129] is an appealing approach to prepare thick, high-force-output material actuators from LCEs, but the resolution of DIW patterning is limited by rheological constraints. By contrast, the preparation of printed LCEs by two-photon polymerization methods[106,107,130] is a powerful means to fabricating microscale devices, with alignment enforced by an external field. However, two-photon polymerization is, in practice, limited to the preparation of small patterned areas. DLP has further

been applied for voxelated molecular patterning in 3D freeforms[103], and, thus, we expect to soon see demonstrations of other 3D printing methods for the preparation of LCEs with microscale features.

Actinic energy inputs

LCEs have the potential to serve as low-density, soft actuators in robotic applications[1], owing to their compelling linear and 3D deformations under load. The magnitude of the force output of actuators made of LCEs by layering[33], interpenetrating networks[131], nanocomposites[132] or 3D printing[121] can reach >20 J kg^{-1}. However, current methods to introduce stimuli for the actuation of LCEs may be a limiting factor for implementations that require a high-frequency response. Thermotropic actuation of LCEs is, by far, the most common approach. Accordingly, the frequency of actuation depends on the rate of heat transfer and dissipation, which, in turn, depend on material thickness and thermal conductivity. Extending thermal actuation to electrothermal[133] (for example, Joule heating) or photothermal[134–136] mechanisms would require thermal monitoring feedback inputs or environmental stabilization to enable practical control of these materials as actuators.

Photochemical events, such as the isomerization of azobenzene, are very rapid at the molecular level[137]. However, employing photoisomerization of azobenzene to generate phototropic actuation of LCEs is typically slow[25,138]. Inherently, azobenzene-functionalized LCEs have a trade-off that must be balanced to use these materials as actuators. Increasing the concentration of azobenzene can increase the magnitude of the photoinduced disruption of order, which correlates with the magnitude of the strain. However, increasing the concentration of azobenzene (or other absorbing medium) also limits the material thickness that can be actuated or increase the time necessary to fully convert the isomeric form of azobenzene in the material from *trans* to *cis*[139]. Electromechanical actuation of LCEs has appealing advantages for soft robotics[29–31]. Electrical power is readily available from small and low-density lithium polymer batteries. In addition, in some cases, for example, in LCE nanocomposites[30,31], the field strength to induce 3D deformation is small (1–2 V μm^{-1}). LCEs have also been subject to electrostriction by Maxwell stresses introduced onto the material by flexible electrodes[29]. Here, the mechanism of electromechanical actuation of LCEs is analogous to dielectric elastomer actuators.

Functional implementations

de Gennes suggested that the mechanical response of LCEs emulates the performance of muscle fibres[3]. Indeed, LCEs can achieve reversible deformations of >400% strain, capable of lifting considerable loads[19]. A largely unexplored path of research is the preparation and implementation of LCE fibres[132,140,141]. The fibres could be geometrically combined, analogous to muscle fibres, to further amplify the force output. These linear actuators could be distributed in soft robotic devices and locally addressed to enable dexterity in function. 3D deformations, enabled by patterning the director orientation of LCEs by directed self-assembly or 3D printing, are also being considered for their potential as 'push' actuators, as well as reconfigurable topographical surfaces. Extruded LCE filaments lock in spatially programmed alignment within a single layer that is an order of magnitude thicker than LCEs prepared by other methods. The force outputs of LCE actuators scale with aligned LCE thickness, which is a potential advantage to prepare LCE actuators by 3D-printing.

Local manipulation of the deformation mechanics of flexible or stretchable substrates could enhance the ruggedness and robustness of flexible hybrid electronic devices[46]. For example, serpentine wires can be used to accommodate deformation and minimize the impact of stress-induced failures of electrode traces[142,143]. The nonlinear and orientation-dependent deformation of LCEs could also be exploited to prepare monolithic substrates for these devices[39,44,45]. For example, a device based on LCEs can withstand high mechanical forces that would typically be catastrophic, and survive by dissipating and localizing the mechanical inputs[39]. The mechanical properties of LCEs have also been investigated in relation to the dissipation of impact or vibration. For example, porous LCE compositions have been explored for implementation in orthopaedic implants[144] or as foams in helmets[145], with the aim to blunt the impact and reduce trauma from head-to-head collisions in American football and other sports.

The nascent anisotropy of LCEs could further be used to pattern the growth of cellular tissues[146,147]. Various cell types, including fibroblasts[17,148], cardiomyocytes[16], myoblasts[149–151] and neurons[152], adhere to and can be propagated on the surface of LCE substrates, which has sparked an interest in the influence of director orientation on cell migration and tissue culture. The potential convergence of 3D printing, LCE materials, chemistry and these 2D studies may provide opportunities to prepare 3D hierarchically aligned tissues.

The recent resurgence of LCEs as responsive materials has been greatly enabled by advances in synthetic methods and materials processing approaches, paving the way for functional applications, from robotics to medicine to consumer products.

Published online 9 September 2021

1. McCracken, J. M., Donovan, B. R. & White, T. J. Materials as machines. *Adv. Mater.* **32**, 1906544 (2020).
2. de Gennes, P. G. Possibilites offertes par la reticulation de polymeres en presence d'un cristal liquide. *Phys. Lett. A* **28**, 725–726 (1969).
3. de Gennes, P. G. A semi-fast artificial muscle. *C. R. Acad. Sci. Ser. IIB Mech. Phys. Chem. Astron.* **324**, 343–348 (1997).
4. Finkelmann, H. & Rehage, G. Investigations on liquid crystalline polysiloxanes, 1. Synthesis and characterization of linear polymers. *Makromol. Chem. Rapid Commun.* **1**, 31–34 (1980).
5. Finkelmann, H., Kock, H.-J. & Rehage, G. Investigations on liquid crystalline polysiloxanes 3. Liquid crystalline elastomers — a new type of liquid crystalline material. *Makromol. Chem. Rapid Commun.* **2**, 317–322 (1981).
6. Portugall, M., Ringsdorf, H. & Zentel, R. Synthesis and phase behaviour of liquid crystalline polyacrylates. *Makromol. Chem.* **183**, 2311–2321 (1982).
7. Küpfer, J. & Finkelmann, H. Nematic liquid single crystal elastomers. *Makromol. Chem. Rapid Commun.* **12**, 717–726 (1991).
This paper introduces mechanical alignment as a means to enforcing uniaxial alignment to LCEs.
8. Finkelmann, H., Kundler, L., Terentjev, E. M. & Warner, M. Critical stripe-domain instability of nematic elastomers. *J. Phys. II* **7**, 1050–1069 (1997).
9. Warner, M. & Terentjev, E. M. *Liquid Crystal Elastomers* (Oxford Univ. Press, 2003).

10. DeSimone, A. & Teresi, L. Elastic energies for nematic elastomers. *Eur. Phys. J. E* **29**, 191–204 (2009).
11. White, T. J. & Broer, D. J. Programmable and adaptive mechanics with liquid crystal polymer networks and elastomers. *Nat. Mater.* **14**, 1087–1098 (2015).
12. Ware, T. H., McConney, M. E., Wie, J. J., Tondiglia, V. P. & White, T. J. Voxelated liquid crystal elastomers. *Science* **347**, 982–984 (2015).
This paper reports the development of aza-Michael addition reaction to prepare LCEs amenable to surface-enforced alignment.
13. Yakacki, C. M. et al. Tailorable and programmable liquid-crystalline elastomers using a two-stage thiol–acrylate reaction. *RSC Adv.* **5**, 18997–19001 (2015).
This paper introduces the widely used thiol-Michael reaction to prepare LCEs by mechanical alignment.
14. Kotikian, A. et al. Untethered soft robotic matter with passive control of shape morphing and propulsion. *Sci. Robot.* **4**, eaax7044 (2019).
15. Brannum, M. T. et al. Light control with liquid crystalline elastomers. *Adv. Opt. Mater.* **7**, 1801683 (2019).
16. Ferrantini, C. et al. Development of light-responsive liquid crystalline elastomers to assist cardiac contraction. *Circ. Res.* **124**, e44–e54 (2019).
17. Turiv, T. et al. Topology control of human fibroblast cells monolayer by liquid crystal elastomer. *Sci. Adv.* **6**, eaaz6485 (2020).
18. Iseki, S. Liquid crystalline elastomer precursor and liquid crystalline elastomer. *J. Polym. Sci.* **55**, 395–411 (2019).
19. Wermter, H. & Finkelmann, H. Liquid crystalline elastomers as artificial muscles. *E-Polym.* **1**, 013 (2001).
20. Ware, T. H. H. & White, T. J. J. Programmed liquid crystal elastomers with tunable actuation strain. *Polym. Chem.* **6**, 4835–4844 (2015).
21. Dong, L. & Zhao, Y. Photothermally driven liquid crystal polymer actuators. *Mater. Chem. Front.* **2**, 1932–1943 (2018).
22. Winkler, M., Kaiser, A., Krause, S., Finkelmann, H. & Schmidt, A. M. Liquid crystal elastomers with magnetic actuation. *Macromol. Symp.* **291–292**, 186–192 (2010).
23. Finkelmann, H. & Shahinpoor, M. Electrically controllable liquid crystal elastomer-graphite composite artifical muscles. *Smart Struct. Mater.* **4695**, 459–464 (2002).
24. Courty, S., Mine, J., Tajbakhsh, A. R. & Terentjev, E. M. Nematic elastomers with aligned carbon nanotubes: New electromechanical actuators. *Europhys. Lett.* **64**, 654–660 (2003).
25. Finkelmann, H., Nishikawa, E., Pereira, G. G. & Warner, M. A new opto-mechanical effect in solids. *Phys. Rev. Lett.* **87**, 015501 (2001).
This paper demonstrates phototropic disruption of order in LCEs prepared with covalent attachment of azobenzene groups.
26. Kosa, T. et al. Light-induced liquid crystallinity. *Nature* **485**, 347–349 (2012).
27. Corbett, D. & Warner, M. Changing liquid crystal elastomer ordering with light–a route to opto-mechanically responsive materials. *Liq. Cryst.* **36**, 1263–1280 (2009).
28. Ringsdorf, H. & Zentel, R. Liquid crystalline side chain polymers and their behaviour in the electric field. *Makromol. Chem.* **183**, 1245–1256 (1982).
29. Davidson, Z. S. et al. Monolithic shape-programmable dielectric liquid crystal elastomer actuators. *Sci. Adv.* **5**, eaay0855 (2019).
30. Guin, T. et al. Electrical control of shape in voxelated liquid crystalline polymer nanocomposites. *ACS Appl. Mater. Interfaces* **10**, 1187–1194 (2018).
31. Guin, T. et al. Tunable electromechanical liquid crystal elastomer actuators. *Adv. Intell. Syst.* **2**, 2000022 (2020).
32. Modes, C. & Warner, M. Shape-programmable materials. *Phys. Today* **69**, 32–38 (2016).
33. Guin, T. et al. Layered liquid crystal elastomer actuators. *Nat. Commun.* **9**, 2531 (2018).
34. Kim, H. et al. Responsive, 3D electronics enabled by liquid crystal elastomer substrates. *ACS Appl. Mater. Interfaces* **11**, 19506–19513 (2019).
35. Flory, P. J. Molecular theory of rubber elasticity. *Polymer* **20**, 1317–1320 (1979).
36. Biggins, J. S., Warner, M. & Bhattacharya, K. Supersoft elasticity in polydomain nematic elastomers. *Phys. Rev. Lett.* **103**, 037802 (2009).
37. Terentjev, E. M. Liquid-crystalline elastomers. *J. Phys. Condens. Matter* **11**, R239 (1999).
38. Finkelmann, H., Greve, A. & Warner, M. The elastic anisotropy of nematic elastomers. *Eur. Phys. J. E* **5**, 281–293 (2001).
39. Auguste, A. D. et al. Enabling and localizing omnidirectional nonlinear deformation in liquid crystalline elastomers. *Adv. Mater.* **30**, 1802438 (2018).
40. Urayama, K., Kohmon, E., Kojima, M. & Takigawa, T. Polydomain–monodomain transition of randomly disordered nematic elastomers with different cross-linking histories. *Macromolecules* **42**, 4084–4089 (2009).
41. Biggins, J. S., Warner, M. & Bhattacharya, K. Elasticity of polydomain liquid crystal elastomers. *J. Mech. Phys. Solids* **60**, 573–590 (2012).
42. Donovan, B. R., Fowler, H. E., Matavulj, V. M. & White, T. J. Mechanotropic elastomers. *Angew. Chem. Int. Ed.* **58**, 13744–13748 (2019).
43. Mistry, D. et al. Isotropic liquid crystal elastomers as exceptional photoelastic strain sensors. *Macromolecules* **53**, 3709–3718 (2020).
44. Ware, T. H., Biggins, J. S., Shick, A. F., Warner, M. & White, T. J. Localized soft elasticity in liquid crystal elastomers. *Nat. Commun.* **7**, 10781 (2016).
45. Fowler, H. E., Donovan, B. R., McCracken, J. M., López Jiménez, F. & White, T. J. Localizing genesis in polydomain liquid crystal elastomers. *Soft Matter* **16**, 330–336 (2020).
46. Gong, S., Yap, L. W., Zhu, B. & Cheng, W. Multiscale soft–hard interface design for flexible hybrid electronics. *Adv. Mater.* **32**, 1902278 (2020).
47. Bergmann, G. H. F., Finkelmann, H., Percec, V. & Zhao, M. Liquid-crystalline main-chain elastomers. *Macromol. Rapid Commun.* **18**, 353–360 (1997).
48. Broer, D., Finkelmann, H. & Kondo, K. In-situ photopolymerization of an oriented liquid-crystalline acrylate. *Makromol. Chem.* **189**, 185–194 (1988).
This paper reports the use of diacrylate liquid crystalline monomers to prepare LCNs amenable to surface-enforced alignment.
49. Kim, H., Boothby, J. M., Ramachandran, S., Lee, C. D. & Ware, T. H. Tough, shape-changing materials: crystallized liquid crystal elastomers. *Macromolecules* **50**, 4267–4275 (2017).
50. Kloxin, C. J. & Bowman, C. N. Covalent adaptable networks: Smart, reconfigurable and responsive network systems. *Chem. Soc. Rev.* **42**, 7161–7173 (2013).
51. Pei, Z. et al. Mouldable liquid-crystalline elastomer actuators with exchangeable covalent bonds. *Nat. Mater.* **13**, 36–41 (2014).
This paper demonstrates that LCEs prepared with dynamic covalent chemistry can be reprocessed to enforce alignment after polymerization.
52. Hanzon, D. W. et al. Adaptable liquid crystal elastomers with transesterification-based bond exchange reactions. *Soft Matter* **14**, 951–960 (2018).
53. Chen, Q. et al. Durable liquid-crystalline vitrimer actuators. *Chem. Sci.* **10**, 3025–3030 (2019).
54. Ube, T., Kawasaki, K. & Ikeda, T. Photomobile liquid-crystalline elastomers with rearrangeable networks. *Adv. Mater.* **28**, 8212–8217 (2016).
55. McBride, M. K. et al. A readily programmable, fully reversible shape-switching material. *Sci. Adv.* **4**, eaat4634 (2018).
56. Wang, Z., Tian, H., He, Q. & Cai, S. Reprogrammable, reprocessible, and self-healable liquid crystal elastomer with exchangeable disulfide bonds. *ACS Appl. Mater. Interfaces* **9**, 33119–33128 (2017).
57. Saed, M. O., Gablier, A. & Terentejv, E. M. Liquid crystalline vitrimers with full or partial boronic-ester bond exchange. *Adv. Funct. Mater.* **30**, 1906458 (2020).
58. Wen, Z. et al. Reconfigurable LC elastomers: using a thermally programmable monodomain to access two-way free-standing multiple shape memory polymers. *Macromolecules* **51**, 5812–5819 (2018).
59. Saed, M. O. & Terentjev, E. M. Siloxane crosslinks with dynamic bond exchange enable shape programming in liquid-crystalline elastomers. *Sci. Rep.* **10**, 6609 (2020).
60. Scheutz, G. M., Lessard, J. J., Sims, M. B. & Sumerlin, B. S. Adaptable crosslinks in polymeric materials: resolving the intersection of thermoplastics and thermosets. *J. Am. Chem. Soc.* **141**, 16181–16196 (2019).
61. Mukherjee, S., Cash, J. J. & Sumerlin, B. S. in *Dynamic Covalent Chemistry: Principles, Reactions, and Applications* Ch. 8 (eds Zhang, W. & Jin., Y.) 321–358 (Wiley, 2017).
62. Kumar, S., Kim, J. H. & Shi, Y. What aligns liquid crystals on solid substrates? The role of surface roughness anisotropy. *Phys. Rev. Lett.* **94**, 077803 (2005).
63. Kowalski, B. A., Tondiglia, V. P., Guin, T. & White, T. J. Voxel resolution in the directed self-assembly of liquid crystal polymer networks and elastomers. *Soft Matter* **13**, 4335–4340 (2017).
64. Harris, K. D. et al. Large amplitude light-induced motion in high elastic modulus polymer actuators. *J. Mater. Chem.* **15**, 5043–5048 (2005).
65. Mol, G. N., Harris, K. D., Bastiaansen, C. W. M. & Broer, D. J. Thermo-mechanical responses of liquid-crystal networks with a splayed molecular organization. *Adv. Funct. Mater.* **15**, 1155–1159 (2005).
66. Broer, D., Boven, J., Mol, G. & Challa, G. In-situ photopolymerization of oriented liquid-crystalline acrylates. III: Oriented polymer networks from a mesogenic diacrylate. *Makromol. Chem.* **190**, 2255–2268 (1989).
67. Safranski, D. L., Lesniewski, M. A., Caspersen, B. S., Uriarte, V. M. & Gall, K. The effect of chemistry on the polymerization, thermo-mechanical properties and degradation rate of poly(β-amino ester) networks. *Polymer* **51**, 3130–3138 (2010).
68. Lynn, D. M. & Langer, R. Degradable poly(β-amino esters): Synthesis, characterization, and self-assembly with plasmid DNA. *J. Am. Chem. Soc.* **122**, 10761–10768 (2000).
69. Ahn, S. K., Ware, T. H., Lee, K. M., Tondiglia, V. P. & White, T. J. Photoinduced topographical feature development in blueprinted azobenzene-functionalized liquid crystalline elastomers. *Adv. Funct. Mater.* **26**, 5819–5826 (2016).
70. Hotta, A. & Terentjev, E. M. Long-time stress relaxation in polyacrylate nematic liquid crystalline elastomers. *J. Phys. Condens. Matter* **13**, 11453–11464 (2001).
71. Ware, T. H., Perry, Z. P., Middleton, C. M., Iacono, S. T. & White, T. J. Programmable liquid crystal elastomers prepared by thiol–ene photopolymerization. *ACS Macro Lett.* **4**, 942–946 (2015).
72. Godman, N. P., Kowalski, B. A., Auguste, A. D., Koerner, H. & White, T. J. Synthesis of elastomeric liquid crystalline polymer networks via chain transfer. *ACS Macro Lett.* **6**, 1290–1295 (2017).
73. Hoyle, C. et al. Thiol-enes: fast curing systems with exceptional properties. *Radtech Eur.* **5**, 2–6 (2005).
74. Jiang, L. et al. Radical polymerization in the presence of chain transfer monomer: An approach to branched vinyl polymers. *Macromolecules* **45**, 4092–4100 (2012).
75. Brannum, M. T. et al. Deformation and elastic recovery of acrylate-based liquid crystalline elastomers. *Macromolecules* **52**, 8248–8255 (2019).
76. Schadt, M. Liquid crystal displays, LC-materials and LPP photo-alignment. *Mol. Cryst. Liq. Cryst.* **647**, 253–268 (2017).
77. Chigrinov, V. G., Kozenkov, V. M. & Kwok, H. S. *Photoalignment of Liquid Crystalline Materials: Physics and Applications* Vol. 17 (Wiley, 2008).
78. Weigert, F. Über einen neuen Effekt der Strahlung in lichtempfindlichen Schichten. *Verh. Dtsch. Phys. Ges.* **21**, 479–491 (1919).
79. Seki, T. New strategies and implications for the photoalignment of liquid crystalline polymers. *Polym. J.* **46**, 751–768 (2014).
80. Ichimura, K. Photoalignment of liquid-crystal systems. *Chem. Rev.* **100**, 1847–1873 (2000).
81. Guo, Y. et al. High-resolution and high-throughput plasmonic photopatterning of complex molecular orientations in liquid crystals. *Adv. Mater.* **28**, 2353–2358 (2016).
82. Murray, B. S., Pelcovits, R. A. & Rosenblatt, C. Creating arbitrary arrays of two-dimensional topological defects. *Phys. Rev.* **47**, 777–780 (2014).
83. Xia, Y., Cedillo-Servin, G., Kamien, R. D. & Yang, S. Guided folding of nematic liquid crystal elastomer sheets into 3D via patterned 1D microchannels. *Adv. Mater.* **28**, 9637–9643 (2016).
84. Aharoni, H., Xia, Y., Zhang, X., Kamien, R. D. & Yang, S. Universal inverse design of surfaces with thin nematic elastomer sheets. *Proc. Natl Acad. Sci. USA* **115**, 7206–7211 (2018).
85. Ditter, D. et al. MEMS analogous micro-patterning of thermotropic nematic liquid crystalline elastomer films using a fluorinated photoresist and a hard mask process. *J. Mater. Chem. C* **5**, 12635–12644 (2017).
86. Buguin, A., Li, M. H., Silberzan, P., Ladoux, B. & Keller, P. Micro-actuators: When artificial muscles made of nematic liquid crystal elastomers meet soft lithography. *J. Am. Chem. Soc.* **128**, 1088–1089 (2006).

87. Kossyrev, P. A., Qi, J., Priezjev, N. V., Pelcovits, R. A. & Crawford, G. P. Virtual surfaces, director domains, and the Fréedericksz transition in polymer-stabilized nematic liquid crystals. *Appl. Phys. Lett.* **81**, 2986–2988 (2002).
88. Liu, D., Bastiaansen, C. W. M., Den Toonder, J. M. J. & Broer, D. J. Photo-switchable surface topologies in chiral nematic coatings. *Angew. Chem. Int. Ed.* **51**, 892–896 (2012).
89. Gebhard, E. & Zentel, R. Ferroelectric liquid crystalline elastomers, 2. Variation of mesogens and network density. *Macromol. Chem. Phys.* **201**, 911–922 (2000).
90. Spillmann, C. M., Ratna, B. R. & Naciri, J. Anisotropic actuation in electroclinic liquid crystal elastomers. *Appl. Phys. Lett.* **90**, 021911 (2007).
91. Rogez, D. & Martinoty, P. Mechanical properties of monodomain nematic side-chain liquid-crystalline elastomers with homeotropic and in-plane orientation of the director. *Eur. Phys. J. E* **34**, 69 (2011).
92. Ge, S. J. et al. A homeotropic main-chain tolane-type liquid crystal elastomer film exhibiting high anisotropic thermal conductivity. *Soft Matter* **13**, 5463–5468 (2017).
93. Brömmel, F. et al. Orientation behaviour of the minor director of homeotropically oriented nematic elastomers in mechanical fields. *Soft Matter* **9**, 2646–2651 (2013).
94. Fréedericksz, V. & Repiewa, A. Theoretisches und Experimentelles zur Frage nach der Natur der anisotropen Flüssigkeiten. *Z. Phys.* **42**, 532–546 (1927).
95. Fréedericksz, V. & Zolina, V. Forces causing the orientation of an anisotropic liquid. *Trans. Faraday Soc.* **29**, 919–930 (1933).
96. Ibrahim, I. H. & Haase, W. Molecular properties of some nematic liquids. I. Magnetic susceptibility anisotropy and order parameter. *J. Phys. Colloq.* **40**, C3-164–C3-168 (1979).
97. Pohl, L., Eidenschink, R., Krause, J. & Weber, G. Nematic liquid crystals with positive dielectric and negative diamagnetic anisotropy. *Phys. Lett. A* **62**, 169–172 (1978).
98. Legge, C. H., Davis, F. J. & Mitchell, G. R. Memory effects in liquid crystal elastomers. *J. Phys. II* **1**, 1253–1261 (1991).
99. Schuhladen, S. et al. Iris-like tunable aperture employing liquid-crystal elastomers. *Adv. Mater.* **26**, 7247–7251 (2014).
100. Li, M. H., Keller, P., Yang, J. & Albouy, P. A. An artificial muscle with lamellar structure based on a nematic triblock copolymer. *Adv. Mater.* **16**, 1922–1925 (2004).
101. Yao, Y. et al. Multiresponsive polymeric microstructures with encoded predetermined and self-regulated deformability. *Proc. Natl Acad. Sci. USA* **115**, 12950–12955 (2018).
102. Cui, J. et al. Bioinspired actuated adhesive patterns of liquid crystalline elastomers. *Adv. Mater.* **24**, 4601–4604 (2012).
103. Tabrizi, M., Ware, T. H. & Shankar, M. R. Voxelated molecular patterning in three-dimensional freeforms. *ACS Appl. Mater. Interfaces* **11**, 28236–28245 (2019).
104. Van Oosten, C. L., Bastiaansen, C. W. M. & Broer, D. J. Printed artificial cilia from liquid-crystal network actuators modularly driven by light. *Nat. Mater.* **8**, 677–682 (2009).
105. Zeng, H. et al. Light-fueled microscopic walkers. *Adv. Mater.* **27**, 3883–3887 (2015).
106. Zeng, H. et al. High-resolution 3D direct laser writing for liquid-crystalline elastomer microstructures. *Adv. Mater.* **26**, 2319–2322 (2014).
107. McCracken, J. M. et al. Microstructured photopolymerization of liquid crystalline elastomers in oxygen-rich environments. *Adv. Funct. Mater.* **29**, 1903761 (2019).
108. Wissbrun, K. F. Rheology of rod-like polymers in the liquid crystalline state. *J. Rheol.* **25**, 619–662 (1981).
109. Rey, A. D. & Tsuji, T. Recent advances in theoretical liquid crystal rheology. *Macromol. Theory Simul.* **7**, 623–639 (1998).
110. Sydney Gladman, A., Matsumoto, E. A., Nuzzo, R. G., Mahadevan, L. & Lewis, J. A. Biomimetic 4D printing. *Nat. Mater.* **15**, 413–418 (2016).
111. M'Barki, A., Bocquet, L. & Stevenson, A. Linking rheology and printability for dense and strong ceramics by direct ink writing. *Sci. Rep.* **7**, 6017 (2017).
112. Redwood, B., Schffer, F. & Garret, B. *The 3D Printing Handbook: Technologies, Design and Applications* (3D Hubs, 2017).
113. Herschel, W. H. & Bulkley, R. Konsistenzmessungen von Gummi-Benzollösungen. *Kolloid Z.* **39**, 291–300 (1926).
114. Lewis, J. A. Direct ink writing of 3D functional materials. *Adv. Funct. Mater.* **16**, 2193–2204 (2006).
115. Leslie, F. M. Some constitutive equations for liquid crystals. *Arch. Ration. Mech. Anal.* **28**, 265–283 (1968).
116. Gelbart, W. M. Molecular theory of nematic liquid crystals. *J. Phys. Chem.* **86**, 4298–4307 (1982).
117. Van Horn, B. L. & Winter, H. H. Dynamics of shear aligning of nematic liquid crystal monodomains. *Rheol. Acta* **39**, 294–300 (2000).
118. Stephen, M. J. & Straley, J. P. Physics of liquid crystals. *Rev. Mod. Phys.* **46**, 617 (1974).
119. Hausmann, M. K. et al. Dynamics of cellulose nanocrystal alignment during 3D printing. *ACS Nano* **12**, 6926–6937 (2018).
120. Ambulo, C. P. et al. Four-dimensional printing of liquid crystal elastomers. *ACS Appl. Mater. Interfaces* **9**, 37332–37339 (2017).
This paper reports the use of direct ink write 3D printing to prepare LCEs with complex orientations.
121. Kotikian, A., Truby, R. L., Boley, J. W., White, T. J. & Lewis, J. A. 3D printing of liquid crystal elastomeric actuators with spatially programed nematic order. *Adv. Mater.* **30**, 1706164 (2018).
122. Roach, D. J., Kuang, X., Yuan, C., Chen, K. & Qi, H. J. Novel ink for ambient condition printing of liquid crystal elastomers for 4D printing. *Smart Mater. Struct.* **27**, 125011 (2018).
123. Hanson Shepherd, J. N. et al. 3D microperiodic hydrogel scaffolds for robust neuronal cultures. *Adv. Funct. Mater.* **21**, 47–54 (2011).
124. Saed, M. O. et al. Molecularly-engineered, 4D-printed liquid crystal elastomer actuators. *Adv. Funct. Mater.* **29**, 1806412 (2019).
125. Davidson, E. C., Kotikian, A., Li, S., Aizenberg, J. & Lewis, J. A. 3D printable and reconfigurable liquid crystal elastomers with light-induced shape memory via dynamic bond exchange. *Adv. Mater.* **32**, 1905682 (2020).
126. Shafiq, Y. et al. A reusable battery-free RFID temperature sensor. *IEEE Trans. Antennas Propag.* **67**, 6612–6626 (2019).
127. Shafiq, Y., Henricks, J., Ambulo, C. P., Ware, T. H. & Georgakopoulos, S. V. A passive RFID temperature sensing antenna with liquid crystal elastomer switching. *IEEE Access* **8**, 24443–24456 (2020).
128. Xia, Y., Zhang, X. & Yang, S. Instant locking of molecular ordering in liquid crystal elastomers by oxygen-mediated thiol–acrylate click reactions. *Angew. Chem.* **130**, 5767–5770 (2018).
129. López-Valdeolivas, M., Liu, D., Broer, D. J. & Sánchez-Somolinos, C. 4D printed actuators with soft-robotic functions. *Macromol. Rapid Commun.* **39**, 1700710 (2018).
130. Zeng, H. et al. Alignment engineering in liquid crystalline elastomers: Free-form microstructures with multiple functionalities. *Appl. Phys. Lett.* **106**, 111902 (2015).
131. Lu, H. F., Wang, M., Chen, X. M., Lin, B. P. & Yang, H. Interpenetrating liquid-crystal polyurethane/polyacrylate elastomer with ultrastrong mechanical property. *J. Am. Chem. Soc.* **141**, 14364–14369 (2019).
132. Liu, J. et al. Shaping and locomotion of soft robots using filament actuators made from liquid crystal elastomer–carbon nanotube composites. *Adv. Intell. Syst.* **2**, 1900163 (2020).
133. Kim, H. et al. Intelligently actuating liquid crystal elastomer-carbon nanotube composites. *Adv. Funct. Mater.* **29**, 1905063 (2019).
134. Lahikainen, M., Zeng, H. & Priimagi, A. Reconfigurable photoactuator through synergistic use of photochemical and photothermal effects. *Nat. Commun.* **9**, 4148 (2018).
135. Camacho-Lopez, M., Finkelmann, H., Palffy-Muhoray, P. & Shelley, M. Fast liquid-crystal elastomer swims into the dark. *Nat. Mater.* **3**, 307–310 (2004).
136. Rastogi, P., Njuguna, J. & Kandasubramanian, B. Exploration of elastomeric and polymeric liquid crystals with photothermal actuation: A review. *Eur. Polym. J.* **121**, 109287 (2019).
137. White, T. J. in *Photomechanical Materials, Composites, and Systems: Wireless Transduction of Light into Work* (ed. White, T. J.) 393–403 (Wiley, 2017).
138. Donovan, B. R., Matavulj, V. M., Ahn, S. K., Guin, T. & White, T. J. All-optical control of shape. *Adv. Mater.* **31**, 1805750 (2019).
139. Serra, F. & Terentjev, E. M. Nonlinear dynamics of absorption and photobleaching of dyes. *J. Chem. Phys.* **128**, 224510 (2008).
140. Roach, D. J. et al. Long liquid crystal elastomer fibers with large reversible actuation strains for smart textiles and artificial muscles. *ACS Appl. Mater. Interfaces* **11**, 19514–19521 (2019).
141. Wang, Z., Li, K., He, Q. & Cai, S. A light-powered ultralight tensegrity robot with high deformability and load capacity. *Adv. Mater.* **31**, 1806849 (2019).
142. Ray, T. R. et al. Bio-integrated wearable systems: A comprehensive review. *Chem. Rev.* **119**, 5461–5533 (2019).
143. Khan, Y. et al. A new frontier of printed electronics: flexible hybrid electronics. *Adv. Mater.* **32**, 1905279 (2020).
144. Volpe, R. H., Mistry, D., Patel, V. V., Patel, R. R. & Yakacki, C. M. Dynamically crystalizing liquid-crystal elastomers for an expandable endplate-conforming interbody fusion cage. *Adv. Healthc. Mater.* **9**, 1901136 (2020).
145. Traugutt, N. A. et al. Liquid-crystal-elastomer-based dissipative structures by digital light processing 3D printing. *Adv. Mater.* **32**, 2000797 (2020).
146. Prévôt, M. E. et al. New developments in 3D liquid crystal elastomers scaffolds for tissue engineering: from physical template to responsive substrate. *Proc. SPIE* **10361**, 103610T (2017).
147. Martella, D. & Parmeggiani, C. Advances in cell scaffolds for tissue engineering: the value of liquid crystalline elastomers. *Chem Eur. J.* **24**, 12206–12220 (2018).
148. Chen, J. et al. Spatiotemporal variations of contact stress between liquid-crystal films and fibroblasts guide cell fate and skin regeneration. *Colloids Surf. B* **188**, 110745 (2020).
149. Sharma, A. et al. Biocompatible, biodegradable and porous liquid crystal elastomer scaffolds for spatial cell cultures. *Macromol. Biosci.* **15**, 200–214 (2015).
150. Bera, T. et al. Liquid crystal elastomer microspheres as three-dimensional cell scaffolds supporting the attachment and proliferation of myoblasts. *ACS Appl. Mater. Interfaces* **7**, 14528–14535 (2015).
151. Gao, Y. et al. Biocompatible 3D liquid crystal elastomer cell scaffolds and foams with primary and secondary porous architecture. *ACS Macro Lett.* **5**, 4–9 (2016).
152. Prévôt, M. E. et al. Liquid crystal elastomer foams with elastic properties specifically engineered as biodegradable brain tissue scaffolds. *Soft Matter* **14**, 354–360 (2018).

Acknowledgements
The authors acknowledge the financial support of the Army Research Office (ARO), Defense Advanced Research Projects Agency (DARPA), the Materials and Manufacturing Directorate of the Air Force Research Laboratory (AFRL) and the University of Colorado. H.E.F. acknowledges Graduate Research Fellowship support from the National Science Foundation. K.R.S. acknowledges support from the Department of Defense (DoD) through the National Defense Science and Engineering Graduate (NDSEG) Fellowship Program.

Author contributions
All authors contributed to the preparation of this Review.

Competing interests
The authors declare no competing interests.

Publisher's note
Springer Nature remains neutral with regard to jurisdictional claims in published maps and institutional affiliations.

RELATED LINKS
Impressio.tech: https://www.impressio.tech/